



Thermal properties of the crust and the lithosphere–asthenosphere boundary in the area of Poland from the heat flow variability and seismic data

Jacek Majorowicz^{1,2} · Marcin Polkowski³ · Marek Grad³ 

Received: 30 July 2018 / Accepted: 19 December 2018 / Published online: 5 January 2019
© The Author(s) 2019

Abstract

High-resolution 3D seismic P-wave velocity model of Poland (Grad et al., *Tectonophysics* 666:188–210, 2016) and corrected for paleoclimate heat flow map (Majorowicz and Wybraniec, *Int J Earth Sci* 100(4):881–887, 2011) gridded to a common mesh are used together with four independent thermal models of the crust and upper mantle to calculate heat flow variation with depth and geotherms. Heat flow at Moho depth are calculated and mapped and both confirm large variability with an elevated mantle heat flow (circa 30–40 mW/m²) in the Paleozoic Platform which is some 10–20 mW/m² higher than Moho heat flow in the north-eastern and south-eastern Poland which belong to a variety of tectonic terranes (the oldest Precambrian Craton, younger Cadomian, Trans-European Suture Zone, Carpathians). Temperatures calculated for the crust show consistent pattern: higher temperatures beneath the Paleozoic Platform and lower temperatures beneath the Precambrian and Cadomian units. At 10 km depth this difference is about 150 °C, about 300 °C at 20 km depth, and about 400 °C at 50–60 km. Assuming the calculated isotherm 580 °C as Curie temperature the magnetic crust thickness was determined as 5–10 km only beneath the Polish Basin, circa 20 km in Carpathians, circa 30 km in Sudetes, and 35–40 km beneath the Precambrian and Cadomian units. Such a thick magnetic crust results from a great depth of Curie temperature, thick crystalline crust, and thin sediments. Mantle heat flow variability is mainly correlating with measured surface heat flow and influences geotherms. Calculated thermal LAB depth follows patterns of heat flow and Moho heat flow variability through Poland with thinnest lithosphere in the high surface heat flow and high mantle heat flow areas. Comparison of this thermal LAB depth estimates with seismic data based LAB depth shows general coincidences when Precambrian Craton vs Paleozoic Platform are considered along the P4 seismic experiment data model (circa 190 km depth vs some 90 km depth, respectively). However, significant differences exist in many areas and especially for the SE Poland when compared with map for the whole of Poland compiled from other seismic reported data.

Keywords 3D seismic model of the crust · Heat flow · Geotherms · Magnetic crust · LAB · Central Europe tectonic units

Introduction

The contact between the East European Craton (EEC) and located to SW Paleozoic Platform (PP) is a major geological boundary in Europe (Fig. 1). The nature and structure of

this contact in the area of Poland is considerably less known and mostly hypothetical. This is mostly due to the fact that this zone is largely concealed beneath thick Paleozoic to Cenozoic sediments, particularly in the area of Polish basin and Lublin basin, and in the Carpathians and their foreland. Information about deep structure come from geophysical studies. In this paper, we analyze thermal properties of the crust and upper mantle for the whole area of Poland basing on the seismic structure. Previous studies of the thermo-seismic structure of the crust and lower lithosphere in the contact of the East European Craton and Paleozoic Platform performed in Poland included seismic works (e.g. Grad et al. 2002a, 2007; Guterch et al. 1983, 2015) and heat flow

✉ Marek Grad
mgrad@mimuw.edu.pl

¹ University of Alberta, Edmonton, Canada

² Present Address: Northern Geothermal Consult, Edmonton, Canada

³ Faculty of Physics, Institute of Geophysics, University of Warsaw, Warsaw, Poland

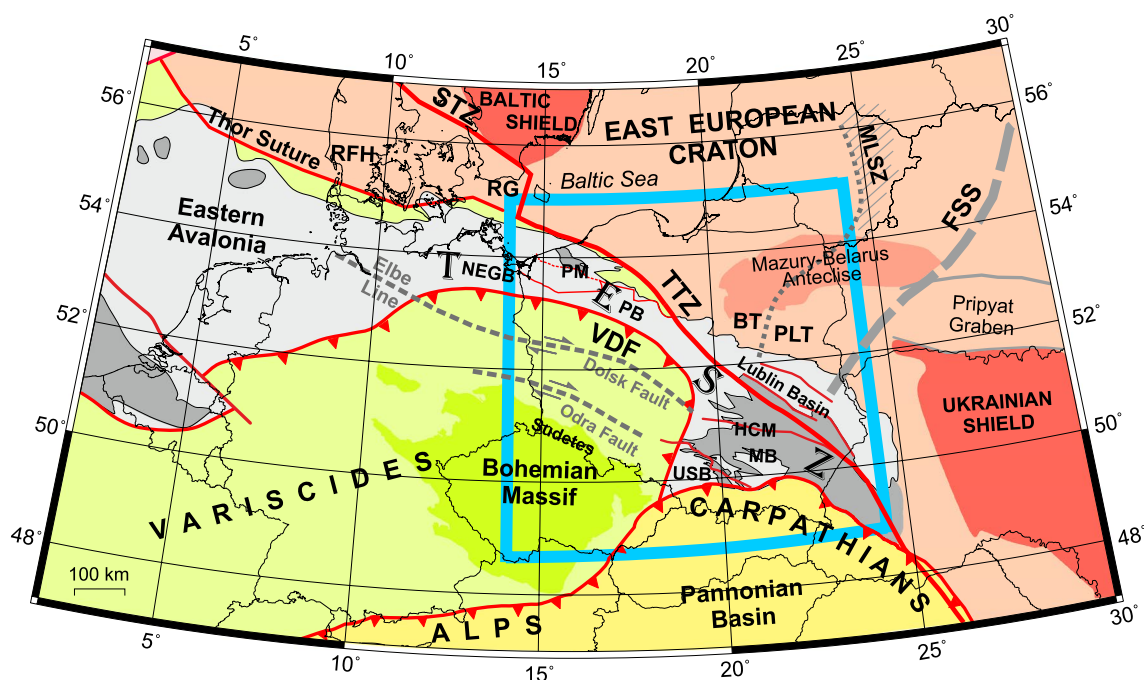


Fig. 1 Tectonic sketch of the pre-Permian Central Europe in the contact of the East European Craton, Variscan and Alpine orogens compiled mainly from Pożaryski and Dembowski (1983), Ziegler (1990), Winchester et al. (2002), Narkiewicz et al. (2011), Cymerman (2007), Skridlaitė et al. (2006), Franke (2014), and Mazur et al. (2015). Blue frame shows location of the study area. *BT* Baltic Terrane; *FSS* Fennoscandia-Sarmatia Suture; *HCM* Holy Cross Moun-

tains; *MB* Małopolska Block; *MLSZ* Mid-Lithuanian Suture Zone; *NEGB* North-Eastern German Basin; *PB* Polish Basin; *PM* Pomerania Massif; *RG* Rønne Graben; *RFH* Ringkobing-Fyn High; *STZ* Sorgenfrei-Tornquist Zone; *TESZ* Trans-European Suture Zone; *TTZ* Teisseyre-Tornquist Zone; *USB* Upper Silesian Block; *VDF* Variscan Deformation Front

studies (e.g. Majorowicz and Plewa 1979; Majorowicz et al. 2003).

Tectonic and geophysical background of the study area

In the area of Poland three large continental scale tectonic units meet together, namely Precambrian East European Craton (EEC) to the northeast, Variscan West European Platform (WEP) terranes to the southwest, and younger Alpine Carpathian arc in the south. Their locations are shown in Fig. 1, together with blue frame showing the area studied in this paper.

The reference structure of the Central Europe is a sharp edge of the East European Craton. In the area of Poland the south-western margin of EEC is marked as Teisseyre-Tornquist Zone (TTZ), which continues to the north as Sorgenfrei-Tornquist Zone (STZ). The term TTZ has previously been a subject to different definitions. Here TTZ describes a zone associated with the southwestern edge of the paleocontinent Baltica (EEC), and STZ is its continuation in Scandinavia (Fig. 1; Teisseyre 1893, Tornquist 1908; Dadlez et al. 2005; Bogdanova et al. 2006). From the very beginning

the TTZ was conceived as a linear feature (fault or fault zone) marking the southwestern boundary of the EEC. Contrarily, the Trans-European Suture Zone (TESZ) is a term coined by Berthelsen (1992) for an assemblage of suspect terranes adjoining the EEC edge from the southwest. It is not a linear structure, but a terrane accretion zone, 100–200 km wide (Fig. 1). In central and north-western Poland the TESZ is boarded by the East European Craton and the Variscan orogeny (Pharaoh 1999, Winchester et al. 2002). Both terms should not be mistaken, as is the case on many maps concerning the problem (Dadlez et al. 2005).

The TTZ/STZ is a major lithospheric structure, which appears to be a deep-seated boundary reaching at least down to a depth of about 200 km as shown by tomographic analysis of shear wave velocity structure of the mantle under Europe (Zielhuis and Nolet 1994; Wilde-Piórko et al. 2002, 2010; Bruneton et al. 2004). Another indication of the deep-seated nature of this zone was obtained from observations of several hundred earthquakes and explosions located in Europe. To explain the observed blockage of energy from regional seismic events by TTZ, the structural anomaly between eastern and western Europe must reach at least down to a depth of about 200 km (Schweitzer 1995). Similar effect was observed for the records of Kaliningrad district

earthquakes (Russia, September 21, 2004). One spectacular observation is that concerning to wave propagation: surface waves propagate extremely far to the north in the Fennoscandian Shield; on the other hand TTZ has some attenuating effect on the seismic waves recorded on the seismograph stations in the west. The macroseismic intensity maps show the same effect (Gregersen et al. 2007).

TTZ/STZ is the longest tectonic feature in Europe separating the old, characterized by thick crust EEC with Paleozoic sedimentary cover from the younger, characterized by thin crust Phanerozoic mobile belts of central and Western Europe (Fig. 2). In the area of Central Europe, the depth of the Moho discontinuity is about 28–36 km beneath Variscides, TESZ and Eastern Avalonia, and 40–48 km beneath the EEC. In the Alpine orogeny thick crust is observed in Alps (> 45 km), while in Pannonian basin and Carpathians crust is thin (< 30 km).

Continental-scale tectonic units of the Central Europe are not clearly correlated with heat flow pattern. Figures 3 and 4 show heat flow map of the Central Europe based on corrected for paleoclimate heat flow data according to Majorowicz and Wybraniec (2011). TTZ is not a clear boundary between low heat flow in the East–North East (mainly Precambrian Platform) and higher heat flow in the West–South West (mainly Paleozoic Platform). Low heat flow zone < 60 mW/m² extends west of TTZ in the Northern Poland and Southern Poland in the Caledonian Pomeranian block and Cadomian block, respectively (Fig. 4). The lowest heat flow values are within Precambrian Platform and shield.

Highest heat flow in the shown part of the heat flow map (Fig. 3) is seen in the rift like Rhine Graben and in the Inner Carpathian Pannonian basin (> 90 mW/m²).

Paleoclimatic effect due to a cold glacial epoch temperatures in Europe, some 10 °C colder than in Holocene, results in a substantial reduction of heat flow at shallow depth. This explains some very low uncorrected heat flow values 20–30 mW/m² in the shields and shallow basin areas of the craton (e.g. Čermák and Bodri 1986). Analysis of the uncorrected and corrected heat flow maps showed that large differences existed in the areas of Baltic and Ukrainian shields, eastern parts of the East European Craton with shallow crystalline basement, orogenic belts like Caledonian and exposed Variscan belts and massifs. The differences between corrected and uncorrected values of heat flow in some cases were significant, particularly for shallow wells, heat flow values were underestimated up to 20 mW/m² (Majorowicz and Wybraniec 2011).

In Poland, heat flow modeling (Majorowicz 2004; Wróblewska and Majorowicz 2008) based on 2D thermo-seismic models along the POLONAISE'97 and CELEBRATION 2000 seismic profiles and use of Rybach (1978) relationship between radiogenic heat production of the crystalline rocks corrected for pressure/temperature found an anomalous zone of elevated mantle heat flow $Q_M > 35$ mW/m² in southwestern Poland in the Variscan forefront and as low as 10–20 mW/m² in the eastern Poland mainly in the Precambrian Platform. However, TESZ does not seem to be a simple dividing boundary. Previously single 1D models

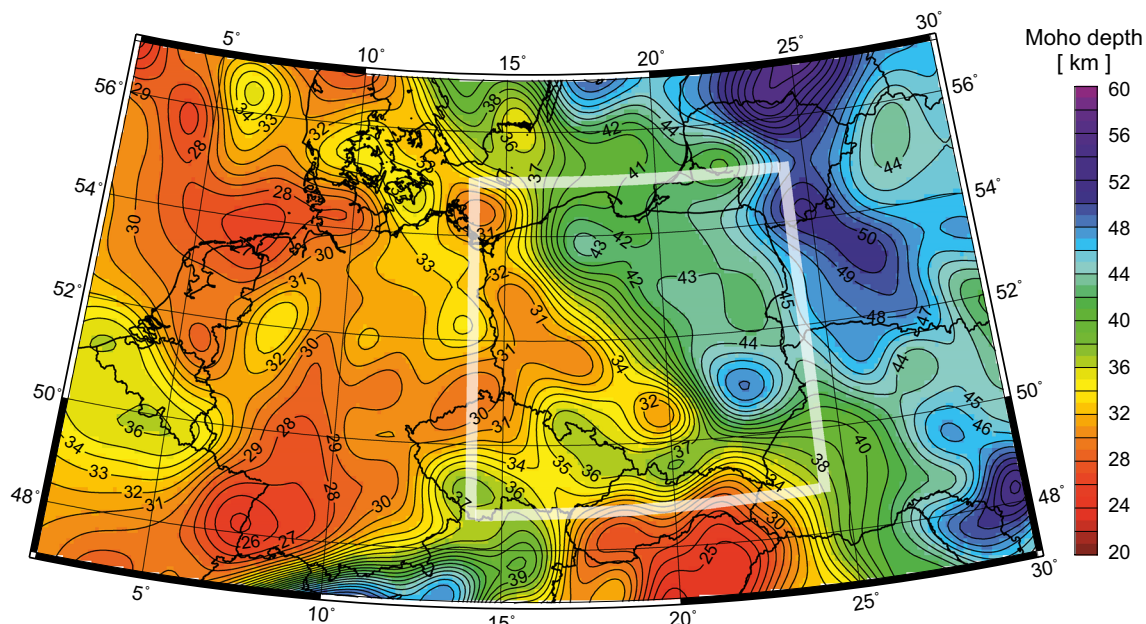


Fig. 2 Moho map of the Central Europe extracted from the Moho depth map of the European Plate (Grad et al. 2009). Grey frame shows location of the study area

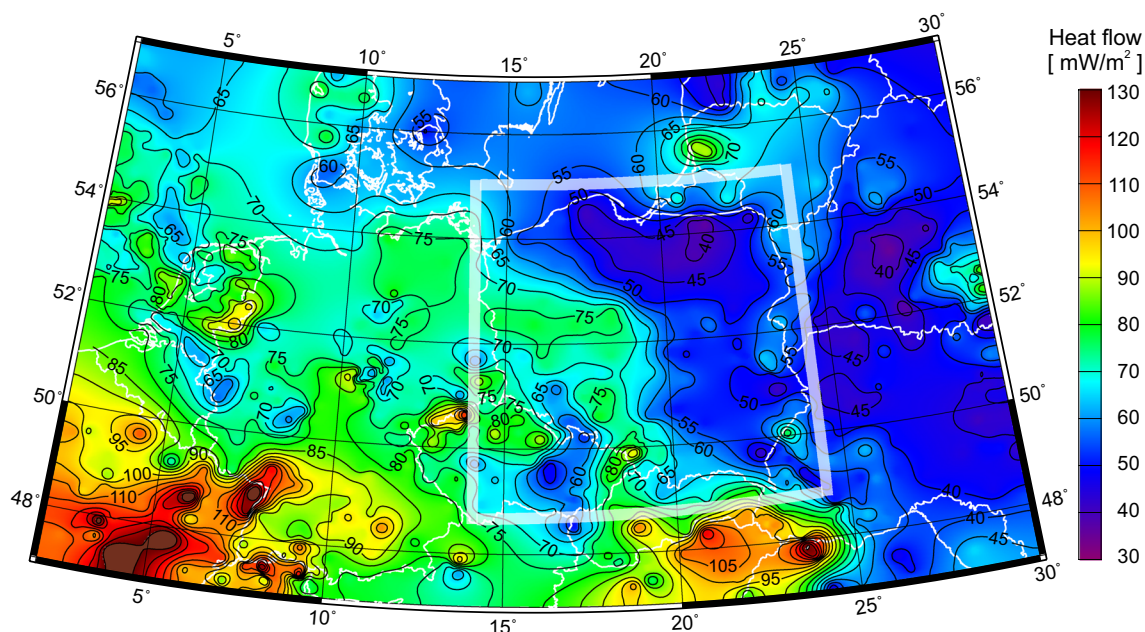


Fig. 3 Central European heat flow map based on corrected for paleoclimate heat flow data according to Majorowicz and Wybraniec (2011). Grey frame shows location of the study area

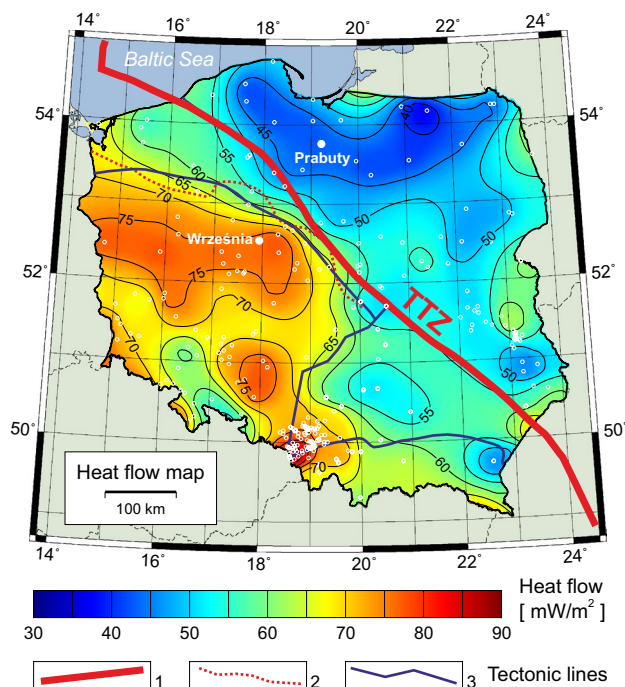


Fig. 4 Heat flow map of Poland based on corrected for paleoclimate heat flow data according to Majorowicz and Wybraniec (2011). White circles show the distribution of boreholes with heat flow data. Big white dots show locations of two test sites Prabuty and Września (see Fig. 8). Tectonic lines: 1—position of the TTTZ in Poland according Narkiewicz et al. (2011); 2—magnetic line, southern margin of the Pomeranian Massif after Królikowski (2006); 3—basement borders after Karnkowski (2008)

based on seismic data showed the same trend (Majorowicz 1978). Such elevated mantle heat flow Q_M coincides with elevated surface heat flow in the same zone (Majorowicz and Wybraniec 2011) and has its continuation towards North-West into Germany, where in the North-Eastern German Basin (NEGB) Q_M is 30–40 mW/m² (Balling 1995; Nordern et al. 2008).

Seismic data and 3D crustal model of Poland

A recently presented high-resolution 3D seismic model for the crust and upper mantle in the area of Poland (Grad et al. 2016) could be useful for further geophysical, including thermal interpretations. The database for the 3D seismic model of Poland and chosen data used in thermal modeling are shown in Fig. 5. Seismic velocities in the sedimentary cover were determined using 1188 deep boreholes with vertical seismic profiling (VSP; Fig. 5a). The basement depth and crustal and uppermost mantle structure were determined from modern seismic profiles (Fig. 5b; Polkowski and Grad 2015; Grad and Polkowski 2016; Grad et al. 2016). Thickness of sediments and Moho depth maps are shown in next figures (Fig. 5c, d, respectively). Seismic model from the topography to depth 60 km includes multilayer sedimentary cover (*TQ* Tertiary and Quaternary, *Cr* Cretaceous, *Ju* Jurassic, *Tr* Triassic, *Pe* Permian, *OP* Old Paleozoic (Pre-Permian), *Fly* Carpathian Flysch), three layer crystalline crust—upper, middle and lower, and uppermost mantle.

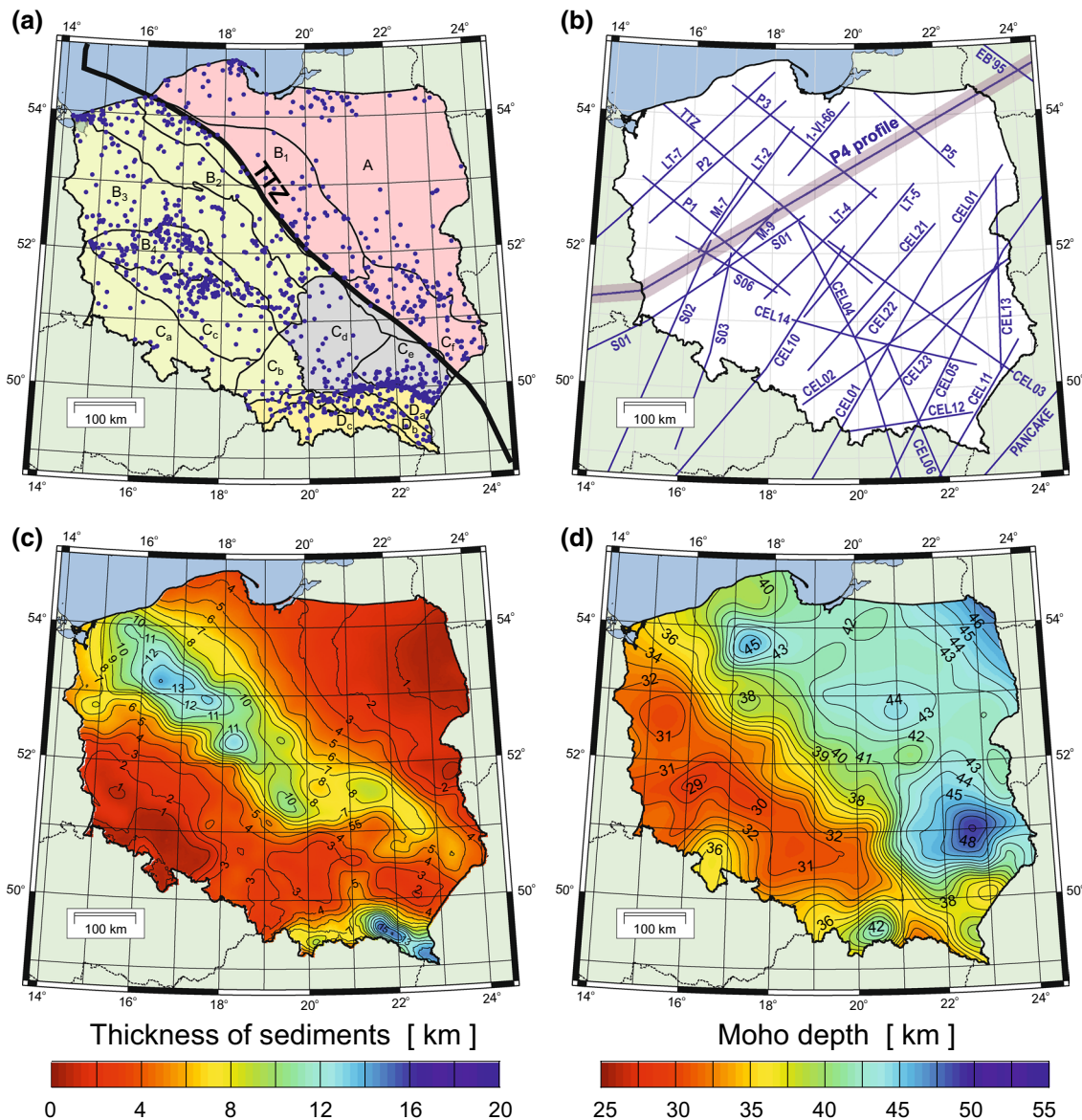


Fig. 5 The database for the seismic model of Poland and data from 3D model used in thermal modeling. **a** Location map of 1188 boreholes with vertical seismic profiling (VSP) on the background of the geological division of Poland, simplified from Sokołowski (1968, 1992). A—east European Craton; B1—marginal synclinorium; B2—Pomorze-Kujawy anticlinorium; B3—Szczecin-Lódź synclinorium; B4—northern fore-Sudetic monocline; Ca—Sudetes and fore-Sudetic block; Cb—Upper Silesian block; Cc—southern fore-Sudetic monocline; Cd—Miechów synclinorium, Goleniów anticlinorium and Holy Cross anticlinorium; Ce—San elevation; Cf—Lublin synclinorium; ; Da—Outer Carpathians; Db—Silesian unit; Dc—Magura unit and Inner Carpathians. TTZ is a SW margin of the East European Craton. Background colors show different basements (Karnkowski 2008): EEC (pink), Cadomian (grey), Variscan (yellow) and Carpathian (orange). **b** Location of modern seismic refraction experiments and profiles used in construction of 3D seismic model of Poland: POLONAISE'97: Guterch et al. (1999); profile P1—Jensen et al. (1999); profile P2—Janik et al. (2002); profile P3—Środa and

POLONAISE Working Group (1999); profile P4—Grad et al. (2003); profile P5—Czuba et al. (2001); CELEBRATION 2000: Guterch et al. (2003); profiles CEL01 and CEL04—Środa et al. (2006); profile CEL02—Malinowski et al. (2005); profile CEL03—Janik et al. (2005); profile CEL05—Grad et al. (2006); profile CEL10—Hrubcová et al. (2008); profiles CEL06, CEL11, CEL12, CEL13, CEL14, CEL21, CEL22, and CEL23—Janik et al. (2009, 2011); SUDETES 2003: Grad et al. (2003); profile S01—Grad et al. (2008); profiles S02, S03, and S06—Majdański et al. (2006); OTHER profiles: LT2, LT4, and LT5—Grad et al. (2005); profile LT7—Guterch et al. (1994); profiles M7 and M9—Grad (1991); profile TTZ—Grad et al. (1999); profile PANCAKE—Starostenko et al. (2013); profile I VI66—Grad et al. (1990); profile EB'95—EUROBRIDGE'95 Seismic Working Group (2001). Highlighted part of the P4 profile shows a location of cross section in Fig. 12. **c** Thickness of sediments in the area of Poland (Grad and Polkowski 2016). **d** Moho depth from 3D seismic model of Poland (Grad et al. 2016)

The 3D seismic model is constructed as rectangular grid in geographic coordinates. Total size of the grid is $631 \times 536 \times 6261$ cells, while size of each cell is $0.01^\circ \times 0.02^\circ \times 10$ m. Area covered by the model spans from 48.7°N to 55.0°N , 13.8°E to 24.5°E and 2600 m.a.s.l. to 60,000 m.b.s.l. Due to limited availability of seismic data outside territory of Poland the model is limited to Polish border and does not provide any information outside it. The size of the model cells was selected to allow representation of complex layer structure (especially in sediments) using only the grid itself. Since the size of the individual grid cell is about $1.1 \text{ km} \times 1.1 \text{ km} \times 10 \text{ m}$ the layers thickness and depth can be tracked up to 10-m accuracy. Since the model does not feature faults, a horizontal resolution of $1.1 \times 1.1 \text{ km}$ is enough to represent structure with the very good amount of detail.

Both thickness of layers and average P-wave velocities show great variations (Grad et al. 2016). In the EEC the thinnest sedimentary cover in the Mazury–Belarus anticline is only 0.3–1 km thick, which increases to 7–8 km along the East European Craton margin, and to 9–12 km in the TESZ. The Variscan domain is characterized by a 1–4 km thick sedimentary cover, while the Carpathians are characterized by very thick sedimentary layers, up to about 20 km. The crystalline crust is differentiated and has a layered structure. In general crustal layers in the EEC are thicker than those in the area of PP. A general decrease in velocity is observed from the older to the younger tectonic domains. The crust beneath the PP is characterized by P-wave velocities of 5.8–6.6 km/s. The upper and middle crusts beneath the EEC are characterized by velocities of 6.1–6.6 km/s, and are underlain by a high velocity lower crust with a velocity of about 7 km/s. Seismic data indicate high-velocity lower part of the crust in the TESZ ($> 7.0 \text{ km/s}$). It is continued towards north-west in Germany, and is interpreted to be due to abundant mafic intrusions (Rabbel et al. 1995; Bayer et al. 2002). The SW limitation of this lower crust is the Elbe line (Aichroth et al. 1992). In the area of Poland the TESZ is associated with a steep dip in the Moho depth. Abrupt transition of the crustal thickness across the TESZ from the 43–45 km thick crust of the EEC to the 28–32 km thick PP crust (Fig. 5d) takes place over a short lateral distance of about 100 km. The slope of the Moho boundary between EEC and WEP corresponds to the axis of the TESZ and reach value of about 10° (Grad et al. 2016). High seismic velocity of the lower crust in the TESZ correlates to the high P-wave velocity (about 8.4 km/s) in the uppermost mantle beneath the Polish Basin. The EEC area is generally characterized by high P-wave velocities ($\sim 8.2 \text{ km/s}$), while the PP area is characterized by velocities of $\sim 8.0 \text{ km/s}$. In the structure of the lower lithosphere in the transition PP–TESZ–EEC seismic reflectors appear as a general

feature at around 10 km depth below Moho, independent of the actual depth to the Moho and sub-Moho seismic velocity (Grad et al. 2002b).

“Ringing reflections” are explained by relatively small-scale heterogeneities beneath the depth interval from circa 90 to 110 km. The seismic reflectivity of the uppermost mantle is stronger beneath the Paleozoic Platform and TESZ than the East European Platform.

Heat flow and thermal parameters

Surface heat flow Q_0 gives information about the thermal state of the Earth’s interior. It is a sum of radiogenic heat production A component of which the largest part comes from the crust plus radiogenic and transient input from below the Moho Q_M . We are using heat flow data based on heat flow determined from continuous temperature–depth $T(z)$ logs and measured thermal conductivity λ from core samples. These older data are in the heat flow database available as an additional supplement to Majorowicz and Wybraniec (2011). Heat flow values were corrected for the effect of glacial–interglacial surface temperature change forcing: maps of Q_0 for the Central Europe is shown in Fig. 3 and map for the investigated Polish area in Fig. 4. In the area of Poland heat flow is low in Precambrian EEC ($\sim 40\text{--}50 \text{ mW/m}^2$), higher in south-eastern Poland where the basement is Cadomian ($\sim 50\text{--}60 \text{ mW/m}^2$), and highest for Variscides with Paleozoic basement ($\sim 60\text{--}80 \text{ mW/m}^2$).

To study thermal state of the Earth’s interior using surface heat flow Q_0 the knowledge of two parameters has a crucial importance: thermal conductivity λ and heat production A for sediments and crystalline rocks.

Thermal conductivity λ for sedimentary rocks, depends on rock composition, maturation, fluid content, temperature, etc. Global values are in wide range of 1–4 $\text{W/m}^\circ\text{C}$. Values of thermal conductivity λ for magmatic rocks are also in wide range and they increase with depth in the crust. According to Moisiejev and Smyslov (1986) the range (and average) values are 1.00–3.85 (2.40) $\text{W/m}^\circ\text{C}$ for acid rocks, 1.38–3.80 (2.31) $\text{W/m}^\circ\text{C}$ for intermediate rocks, 1.59–3.25 (2.45) $\text{W/m}^\circ\text{C}$ for mafic (basic) rocks and 2.30–5.00 (3.42) $\text{W/m}^\circ\text{C}$ for ultramafic rocks.

Nowadays, we have no consistent data for the thermal conductivity λ distribution in the sedimentary cover of the area of Poland. Some data and regional compilations are available, e.g. for Cambrian rocks of the Lublin synclinorium (unit Cf in Fig. 5a), Paleozoic and metamorphic rocks of the southern fore-Sudetic monocline (unit Cc), Permian rocks of the northern fore-Sudetic monocline (unit B4), Cenozoic, Triassic and Carboniferous rocks of the Upper Silesian block (unit Cb), Flysch complex in the Inner Carpathians (unit Dc), as well as chosen magmatic rocks of the

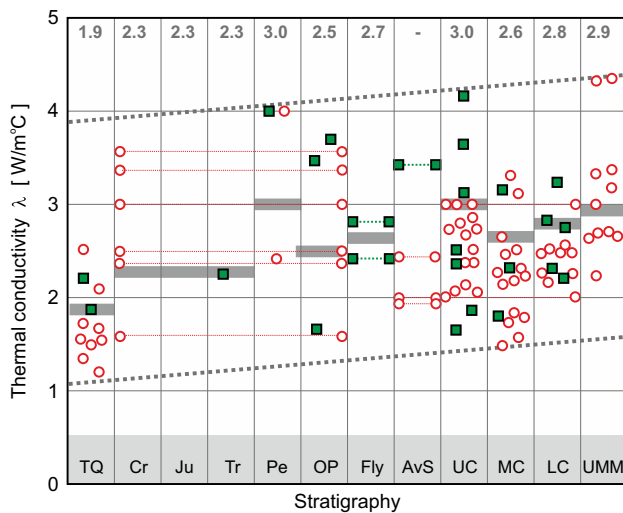


Fig. 6 Experimental thermal conductivity data λ for different stratigraphy: TQ—Tertiary and Quaternary, Cr—Cretaceous, Ju—Jurassic, Tr—Triassic, Pe—Permian, OP—Old Paleozoic (Pre-Permian), Fly—Carpathian Flysch, AvS—average for sediments, UC—Upper Crust, MC—Middle Crust, LC—Lower Crust, UMM—Uppermost Mantle. Green squares are data from the area of Poland compiled from Chmura (1970, 1987), Downorowicz (1983), Plewa (1988), Plewa and Plewa (1992), Bała and Waliczek (2012). Values shown by grey horizontal bars and corresponding values in the top of figure were used for modeling in Model D. For comparison red circles show abroad data compiled from Moisiejev and Smyslov (1986), Eppelbaum et al. (2014), Sharma (2002), Kappelmeyer and Hänel (1974), Dortman (1976), Zeb et al. (2010), Blackwell and Steele (1989), Clark (1966). Grey dotted lines show a range of values, basically between about 1 and 4 W/m°C, slightly increasing with rock depth

crystalline basement. Figure 6 shows experimental thermal conductivity data λ for the area of Poland (green squares) compiled from Chmura (1970, 1987), Downorowicz (1983), Plewa (1988), Plewa and Plewa (1992) and shows for comparison abroad data (red circles) compiled from Moisiejev and Smyslov (1986), Eppelbaum et al. (2014), Sharma (2002), Kappelmeyer and Hänel (1974), Dortman (1976), Zeb et al. (2010), Blackwell and Steele (1989), Clark (1966). Values shown by grey horizontal bars were used for modeling in Model D. Grey dotted lines show a range of values, basically between about 1 and 4 W/m°C, slightly increasing with rock depth/age.

Typical range values of heat production A in the continental crust are different for Archean, Proterozoic and Phanerozoic units being 0.56–0.73, 0.73–0.90, 0.95–1.21 $\mu\text{W}/\text{m}^3$, respectively. Value of A is decreasing with depth, and in average is 1.65, 1.0 and 0.19 $\mu\text{W}/\text{m}^3$ for the upper, middle and lower crust, respectively (e.g. Rudnick and Gao 2003; Jaupart and Mareschal 2003).

Similar as in the case of data for the thermal conductivity λ , nowadays we have no consistent data for the distribution of heat production A for the whole area of Poland.

Individual data and regional compilations are available, e.g. for Triassic and Permian rocks in the northern fore-Sudetic monocline (B4) and in the southern fore-Sudetic monocline (unit Cc), for Flysch, magmatic, acid and intermediate rocks in Carpathians (unit D), Permian and Carboniferous rocks in the Upper Silesian block (unit Cb), acid rocks of the southern fore-Sudetic monocline (unit Cc), acid rocks (granite) in the Sudetes and fore-Sudetic block (unit Ca), Old Paleozoic rocks in the Lublin synclinorium (unit Cf), Cambrian rocks in the East European Craton (unit A), acid, intermediate and crystalline basement rocks in the East European Craton (unit A).

In the case of 3D seismic velocity model, special importance have empirical $A(V_p)$ relations, which permit to calculate heat production A directly from seismic velocity V_p . For the area of Poland such a relation exists for Mesozoic (MP) rocks of the fore-Carpathian region, and is described by formula (Gašior and Przelaskowska 2012):

$$A(V_p) = 5.12e^{-0.4 \cdot V_p}, \quad (1)$$

where radiogenic heat production A is in $\mu\text{W}/\text{m}^3$, and P-wave velocity V_p in km/s.

In the global scale $A(V_p)$ relations for the crystalline crustal rocks are slightly different for Precambrian (Pc) rocks:

$$A(V_p) = 2.0e^{-2.373 \cdot V_p}, \quad (2)$$

and for Phanerozoic (Ph) rocks:

$$A(V_p) = 9.0e^{-2.56 \cdot V_p} \quad (3)$$

where heat production A is in $\mu\text{W}/\text{m}^3$, and V_p is in km/s (e.g. Rybach 1976; Rybach and Buntebarth 1984; Čermák and Bodri 1986). For the velocity $V_p = 6$ km/s the heat production is 1.31 $\mu\text{W}/\text{m}^3$ for the Precambrian (Pc) crust and slightly larger, $A = 1.92$ $\mu\text{W}/\text{m}^3$ for the Phanerozoic (Ph) crust.

Juxtaposition of experimental heat production data is shown in Fig. 7. In Fig. 7a heat production data for different stratigraphy in the area of Poland are shown. Grey lines are average for Precambrian (Pc) and Phanerozoic (Ph) sediments used for modeling in Model D. In Fig. 7b heat production data are shown as a function of V_p seismic velocity. Orange line and orange triangles are data for Carpathian sediments (MP—Meso-Proterozoic rocks; formula 1). Red lines are for Precambrian (Pc) and Phanerozoic (Ph) crystalline lithosphere (formula 2 and 3, respectively). To avoid extraordinary high values of A calculated from 3D seismic model these formulas were limited to 1.5, 1.3 and 2.3 $\mu\text{W}/\text{m}^3$, respectively for formula 1, 2 and 3. These formulas are consistent with corresponding values for East European Craton (pink boxes according to Maj 1991) and for Pannonian Basin (yellow boxes according to Lenkey et al. 2002).

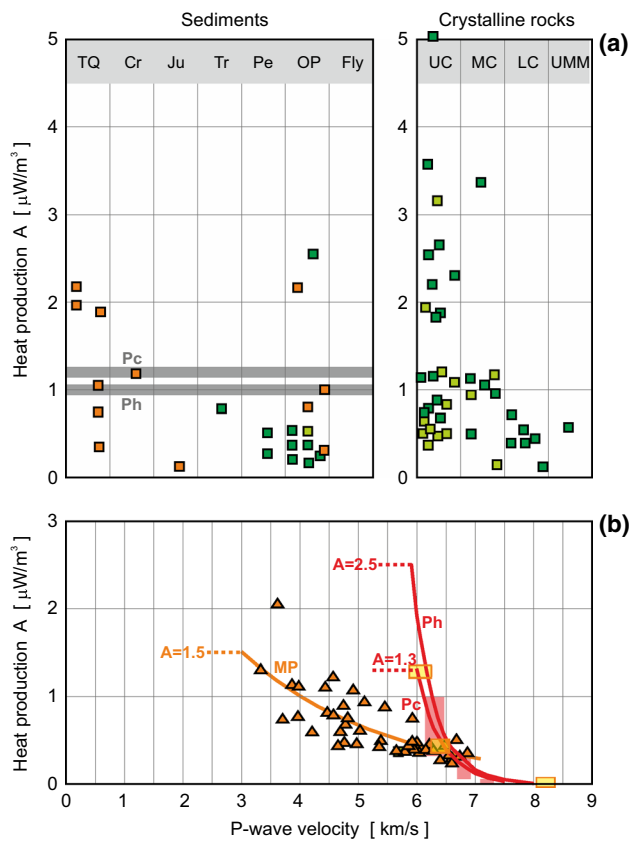


Fig. 7 Experimental heat production data A for sediments and crystalline rocks. **a** Heat production data for different stratigraphy: TQ, Cr, Ju, Tr, Pe, OP, Fly, UC, MC, LC, UMM—abbreviations as in Fig. 6 caption. Green squares are data from Poland (including light green for EEC) and orange squares for Carpathians. Compiled from Plewa and Plewa (1992). Grey lines are average for Precambrian (Pc) and Phanerozoic (Ph) sediments used for modeling in Model D. **b** Heat production data as a function of V_p seismic velocity. Orange line and orange triangles are data for Carpathian sediments (MP—Meso-Proterozoic rocks; formula 1). Red lines are for Precambrian (Pc) and Phanerozoic (Ph) crystalline lithosphere (formula 2 and 3, respectively). Broken lines show a limit of A for three formulas. For comparison are shown data ranges for East European Craton—pink boxes according to Maj (1991) and for Pannonian Basin—yellow boxes according to Lenkey et al. (2002)

Mantle heat flow and geotherms calculations

For a one-dimensional steady state case we have used ‘boot strapping’ method described by Hasterok and Chapman (2011):

$$Q_{i+1} = Q_i - A_i \cdot \Delta z_i, \quad (4)$$

where Q for $i=0$ is surface heat flow Q_0 . Temperature–depth (geotherm) is calculated from:

$$T_{i+1} = T_i + (Q_i/l_i) \cdot \Delta z_i - (A_i/2l_i) / \Delta z_i^2, \quad (5)$$

where A_i and λ_i are intra layers parameters of heat production and rock thermal conductivity, respectively. To calculate geotherm $T(z)$ for the crust and upper mantle down to LAB boundary we take $\Delta z_i = 10$ m, compatible with grid of 3D seismic model. In all modeling a ground surface mean annual temperature $T_0 = 9$ °C was assumed (Plewa 1994; Górecki 2006).

Thermal conductivity of rocks λ is commonly measured in ambient conditions. Changes of λ due to increase of pressure with depth $p(z)$ and temperature with depth $T(z)$ were calculated using equation with empiric constants (Chapman and Furlong 1992, Correia and Safanda 2002; Čermák and Bodri 1986):

$$\lambda(z, T) = \lambda_0(1 + c \cdot z)/(1 + b \cdot (T - 293)), \quad (6)$$

where λ_0 is thermal conductivity at room temperature and atmospheric pressure. Typical values of coefficients c and b for the granitic upper crust are $c = 1.5 \times 10^{-6} \text{ m}^{-1}$, $b = 1.5 \times 10^{-3} \text{ K}^{-1}$. The pressure dependence is the same for the whole crust, i.e. $c = 1.5 \times 10^{-6} \text{ m}^{-1}$. Concerning coefficient b in the middle and lower crust, a constant value of $b = 1.0 \times 10^{-4} \text{ K}^{-1}$ was assumed (Correia and Safanda 2002), and for the mantle, we choose a negative coefficient $b = -2.5 \times 10^{-4} \text{ K}^{-1}$ (Čermák et al. 1989). This reflects a gradually more efficient radiative component of the heat transfer. The pressure dependence of conductivity within the mantle are not well constrained, but considering the uncertainty on the value of λ_0 for the mantle rocks (one can find in the literature values between 2.5 and 4.0 $\text{Wm}^{-1}\text{K}^{-1}$), we neglect the pressure dependence in the mantle.

Heat production A has been assumed for sedimentary cover, the crystalline crust and upper mantle in four models (A, B, C, D) as described below (for their parameters see also Table 1).

Model A For the sedimentary cover heat production A has been assumed as constant (according to Čermák and Bodri 1986). In the crystalline crust and upper mantle the relationship between the A and seismic velocity V_p established for the Precambrian (Pc, formula 2) and Phanerozoic (Ph, formula 3) were used.

Model B For the sedimentary cover heat production A has been assumed as constant (according to Čermák and Bodri 1986). In the crystalline crust and upper mantle we assumed that upper crustal heat flow Q_{UC} generated by radiogenic sources follows the empirical relationship $Q_{UC} = 0.4 \cdot Q_0$, where Q_0 is surface heat flow. This relation was found by Pollack and Chapman (1977) for the continents.

Model C For the sedimentary cover heat production A has been assumed as constant (according to Čermák and Bodri 1986). For the cratonic upper crust we assumed that $Q_{UC} = 0.3 \cdot Q_0$, according to Artemieva and Mooney (2001). For the Phanerozoic tectonic areas $Q_{UC} = 0.4 \cdot Q_0$ was assumed according to Pollack and Chapman (1977).

Table 1 Thermal parameters used for heat flow and temperature modeling for the lithospheric Models A, B, C and D in the territory of Poland

Model	Thermal conductivity λ (W/m°C)	Heat production A ($\mu\text{W}/\text{m}^3$) Heat flow Q (mW/m^2)
A	Whole sedimentary succession: TQ+Cr+Ju+Tr+Pe+OP+Flysch 2.2, UC 3.5, MC 2.5, LC 2.1, UMM 2.5	Sediments: Pc 1.5, Ph 1.0 Crystalline complex: Precambrian (formula 2, Pc, limited et 1.5), other areas (formula 3, Ph, limited et 3.0)
B	Whole sedimentary succession: TQ+Cr+Ju+Tr+Pe+OP+Flysch 2.2, UC 3.5, MC 2.5, LC 2.1, UMM 2.5	Sediments: Pc 1.2, Ph 1.0 Crystalline complex: Precambrian (formula 2, Pc, limited et 1.5), other areas (formula 3, Ph, limited et 3.0)
C	Whole sedimentary succession: TQ+Cr+Ju+Tr+Pe+OP+Flysch 2.2, UC 3.5, MC 2.5, LC 2.1, UMM 2.5	Sediments: Pc 1.2, Ph 1.0 Q in Upper Crust: Precambrian $Q_{UC} = 0.3 \cdot Q_0$, other $Q_{UC} = 0.4 \cdot Q_0$ A in middle + lower crust: Precambrian (formula 2, Pc, limited et 1.5), other areas (formula 3, Ph, limited et 3.0)
D	TQ 1.9, Cr+Ju+Tr 2.3, Pe 3.0, OP 2.5, Flysch 2.7, UC 3.0, MC 2.6, LC 2.8, UMM 2.9 See Fig. 6	Sediments: Pc 1.2, Ph 1.0, Flysch (formula 1, MP, limited et 1.5). Crystalline complex: Precambrian (formula 2, Pc, limited et 1.5), Cadomian (formula 3, Ph, limited et 1.3), other areas (formula 3, Ph, limited et 2.5). Limitations are shown in Fig. 7

In the Models B and C where heat flow/heat production data are not available, we used an empirical relation for reduced heat flow Q_R (heat flow below the upper crustal radiogenic heat flow sources; statistically circa 10 km of the upper crust). Assumed reduced heat flow was used for estimation the upper crustal heat flow contribution $Q_{UC} = Q_0 - Q_R$. According to Pollack (1986) $Q_R = 0.6 \cdot Q_0$, or $Q_R = 0.7 \cdot Q_0$ according to Artemieva and Mooney (2001) for the cratonic areas.

Model D In this model, we used properties of 3D seismic model and local data available for thermal conductivity λ and heat production A for sediments and crystalline rocks (Figs. 6, 7). Thermal conductivity λ values were different for stratigraphic sedimentary layers: for Tertiary and Quaternary 1.9, for Cretaceous + Jurassic + Triassic complex 2.3, for Permian 3.0, for Old Paleozoic 2.5, for Carpathian Flysch 2.7, for Upper Crust 3.0, for Middle Crust 2.6, for Lower Crust 2.8, and for Uppermost Mantle 2.9 (all values in W/m°C). Heat production A values in sediments were differentiated for Precambrian ($1.2 \mu\text{W}/\text{m}^3$) and for Phanerozoic ($1.0 \mu\text{W}/\text{m}^3$) units; in Carpathian Flysch we used $A(V_p)$ formula (1) for Meso-Paleozoic rocks. In the crystalline crust heat production A for Precambrian unit (Pc) were used from formula (2), and for remaining areas according to formula (3). To avoid overestimated A values for lower V_p velocities we used limitations as shown in Fig. 7.

Test results Sample calculations for two locations typical for the low heat flow of the East European Craton (Prabuty, $\phi = 53.77^\circ\text{N}$, $\lambda = 19.22^\circ\text{E}$, $H_{\text{Moho}} = 42.04$ km, $Q_0 = 41.58 \text{ mW}/\text{m}^2$) and high heat flow of the Variscan foreland (Września, $\phi = 52.33^\circ\text{N}$, $\lambda = 17.58^\circ\text{E}$, $H_{\text{Moho}} = 33.14$ km, $Q_0 = 75.99 \text{ mW}/\text{m}^2$) are illustrated in Fig. 8. In the calculations parameters from Model A were taken (see Table 1). For assumed thermal conductivity λ and heat production A heat flow with depth $Q(z)$ and temperature $T(z)$ were

calculated. Geotherms show five approximations: #1 blue curve is based on first approximation with $\lambda(z)$ not depended on temperature/pressure (ambient conditions) and #2, #3, #4, #5 color lines representing next four iterations with $\lambda(z)$ depended on $T(z)$, according to formula (6). Last iteration #5 shows no significant changes comparing to iteration #4, so this geotherm could be used to determination LAB depth, understood as intersection geotherm with mantle adiabat. Consecutive iterations show also influence of temperature dependent $\lambda(z)$ for thermal LAB depth. In the case of hot/thin lithosphere (Września) it is not significant, changing from ~80 km for iteration #1 to ~90 km for iteration #5. In the case of cold/thick lithosphere (Prabuty) it is significant, changing from ~160 km for iteration #1 to ~200 km for iteration #5. These examples show necessity of use temperature dependent $\lambda(z)$, particularly in the case of cold/thick lithosphere.

Spatial and depth distribution of the modeled results

As shown in test sample in previous chapter calculations were done in the same way for the whole territory of Poland. The geometry of sediments, crystalline crust and uppermost mantle was taken from high-resolution 3D seismic P-wave velocity model of Poland (Grad et al. 2016). Corrected for paleoclimate heat flow map (Majorowicz and Wybraniec 2011) and other thermal parameters were gridded to a common mesh and calculations of heat flow $Q(z)$ and geotherms $T(z)$ were made for four independent thermal Models A, B, C and D.

Mantle heat flow Heat flow variations with depth $Q(z)$ were calculated according to formula (4). Mantle heat flow Q_M has been calculated as heat flow at depth of seismically

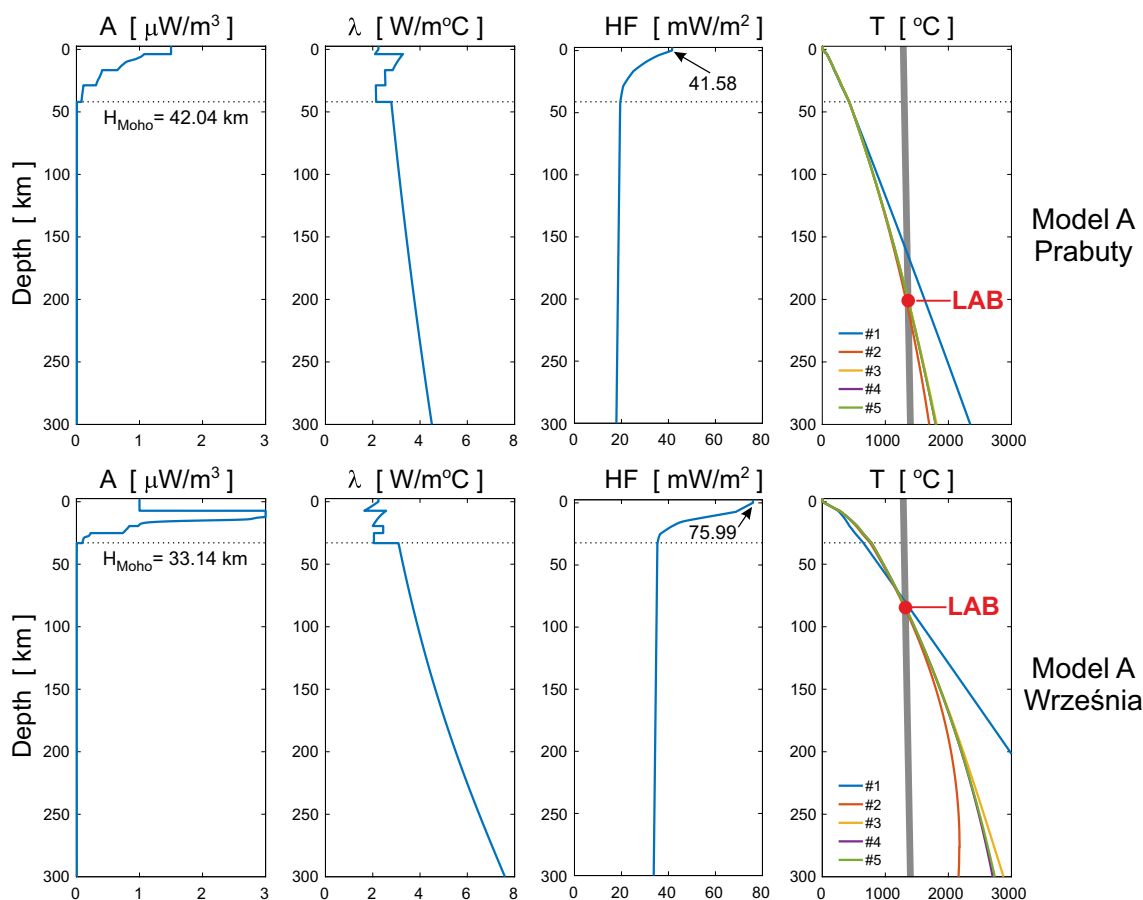


Fig. 8 Illustration of calculated geotherms for Model A in two test sites: Prabuty (top panels) and Września (bottom panels)—for their locations see Fig. 4. Panels show assumed heat production $A(z)$, thermal conductivity $\lambda(z)$, calculated heat flow $Q(z)$ and calculated geotherms $T(z)$ with mantle adiabat. Note: geotherms shown are five approximations: #1 blue curve based on first approximation with $\lambda(z)$ not depended on temperature/pressure (ambient conditions) and

#2, #3, #4, #5 color lines representing next four iterations with $\lambda(z)$ depended on $T(z)$. Thick grey line is mantle adiabat (e.g. MacKenzie and Canil 1999; Hyndman et al. 2009; Hasterok and Chapman 2011). Red dots show thermal LAB—cross point of geotherm (approximation #5) with adiabat. Geotherms and thermal parameters are realistic only up to LAB depth

determined Moho discontinuity and maps of Q_M are shown in Fig. 9. Heat flow Q_M was calculated as the difference between surface heat flow Q_0 and of crustal Q_C and sedimentary Q_S contribution from relation:

$$Q_0 = Q_S + Q_C + Q_M. \quad (7)$$

Heat flow at Moho depth is calculated and mapped and both confirm large variability with an elevated mantle heat flow (circa 30–40 mW/m²) in the Paleozoic Platform which is some 10–20 mW/m² higher than Moho heat flow in the north-eastern and south-eastern Poland which belong to a variety of tectonic terranes (the oldest Precambrian Craton, younger Cadomian, Trans-European Suture Zone and Carpathians). Mantle heat flow variability is mainly correlating with measured surface heat flow and influences geotherms. This tendency is common for all four thermal Models A, B, C and D. In all models the lowest mantle heat flow is

observed for Precambrian cratonic area in northern Poland and in south-eastern Poland for Precambrian and Cadomian units. Low mantle heat flow in south-eastern Poland correlates with area of deepest Moho (> 45 km; Fig. 5d). However, this division does not seem to be a simple dividing boundary.

Temperature Temperature variations with depth $T(z)$ were calculated for assumed thermal conductivity $\lambda(z)$ and heat production $A(z)$ for Models A, B, C and D (Table 1). Temperature at Moho is shown in Fig. 10. For all models the temperature pattern shows many similarities, with difference of about ± 50 °C only. In all models, the lowest Moho temperature 400–500 °C is observed for Precambrian cratonic area in northern Poland and in south-eastern Poland for Precambrian and Cadomian units. On the other hand, the highest Moho temperature 800–900 °C is observed in Central Poland. This hot area correlates well with the location

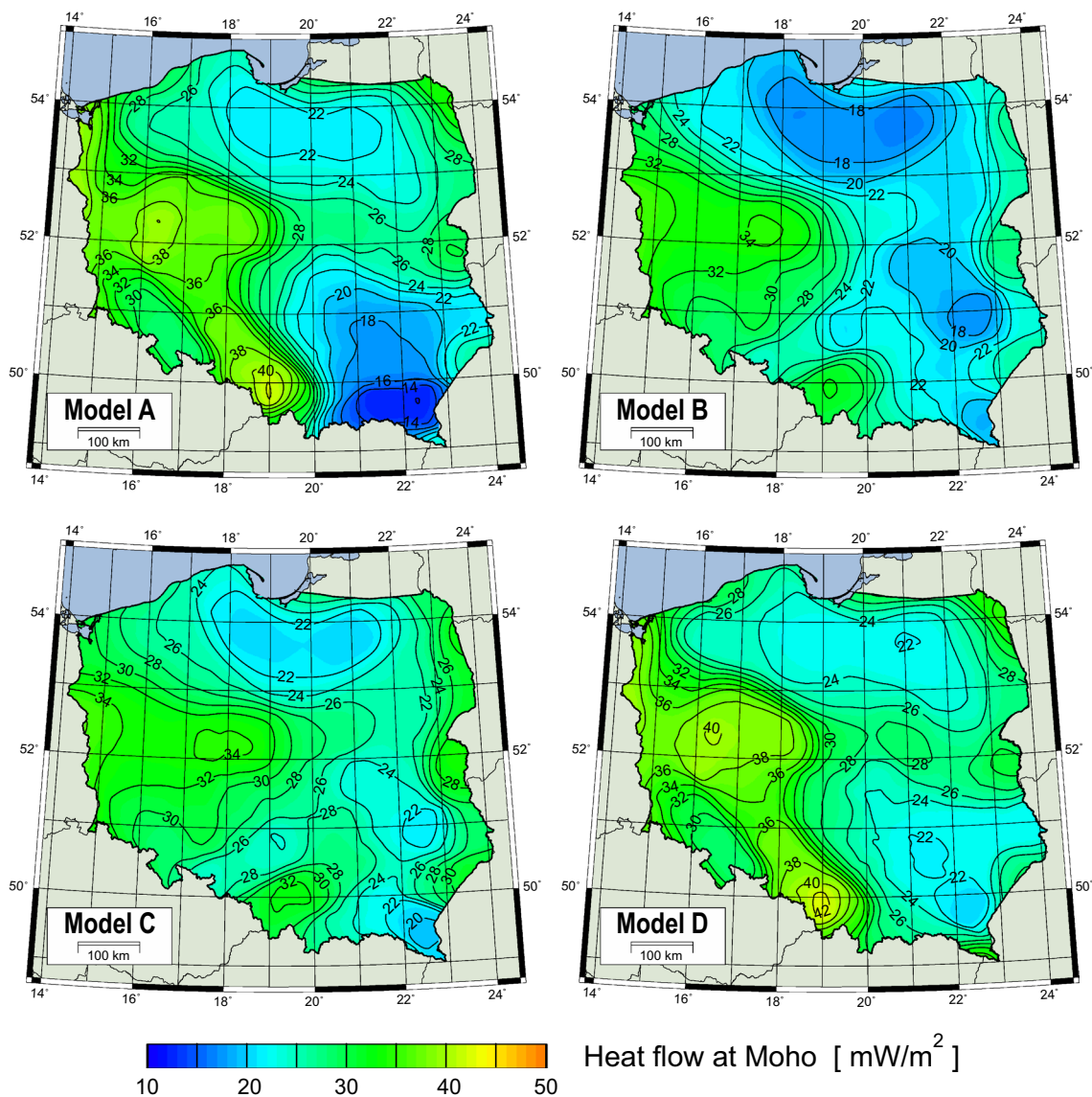


Fig. 9 Moho heat flow Q_M (in mW/m^2) calculated from the observed surface heat flow Q_0 and assumed heat production and thermal conductivity data for four Models: A, B, C and D (compare parameters in Table 1)

of the Polish Basin and high temperature axis has north-west direction, towards the North-Eastern German Basin (compare Fig. 1; Norden et al. 2008; Cacace et al. 2013).

Temperatures calculated for Model D at slices 10, 20, 30, 40, 50 and 60 km are shown in Fig. 11. All they show consistent pattern higher temperatures beneath the Paleozoic Platform and lower temperatures beneath the Precambrian and Cadomian units. At 10 km depth, this difference is about 150 °C, and about 300 °C at 20 km depth. The difference of temperature increases with depth. The depth of 30 km correspond to lower crust of the Paleozoic Platform, and to middle crust of the Precambrian Craton. The next slice at depth of 40 km correspond to uppermost mantle beneath the Paleozoic Platform, and to lower crust of the Precambrian

Craton. In both cases, the temperature difference is about 400 °C, similar to those at 50 and 60 km. It should be mentioned, that such a difference occurs spaced about 300 km only.

Curie temperature and magnetic crust In the study of the crustal magnetism crucial role plays Curie temperature, at which rocks and minerals lose their permanent magnetic properties. For the crustal rocks this temperature is close to 580 °C (e.g. Gasparini et al. 1979), and this value we used for calculation of the Curie temperature T_C depth for Models A, B, C and D (Fig. 12). For all models, results are consistent, showing similar pattern. Relatively shallow depth of T_C is observed beneath the Paleozoic Platform, 15–30 km only. Similar as for Moho temperature this area correlates well

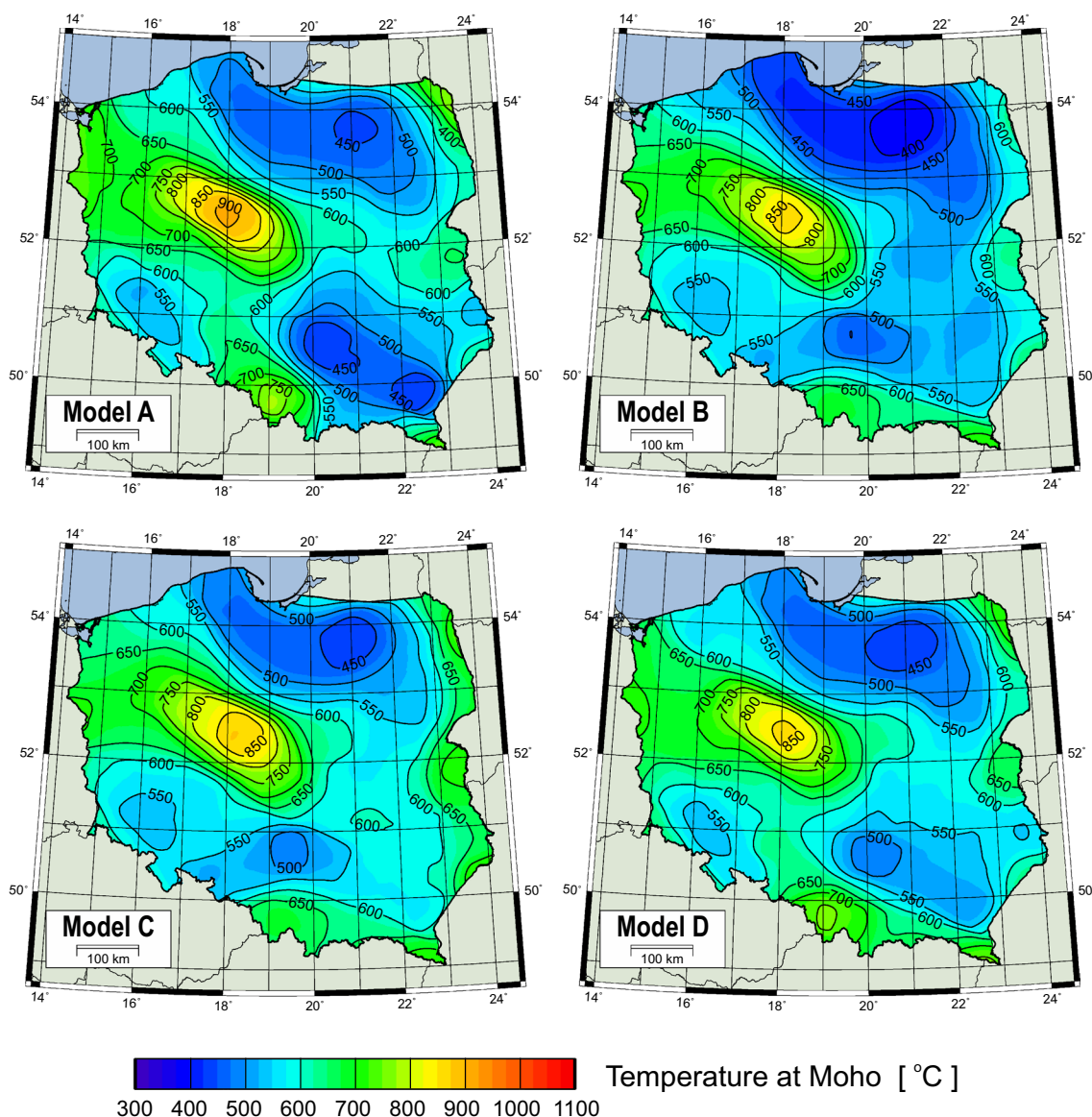


Fig. 10 Moho temperature calculated from the observed surface heat flow Q_0 for assumed heat production and thermal conductivity data in four Models: A, B, C and D (compare parameters in Table 1)

with the location of the Polish Basin and continues towards the north-eastern German Basin. Beneath the Precambrian and Cadomian units the T_C depth is much deeper, reaching 40–55 km.

The knowledge of Curie temperature T_C permits to calculate map of the magnetic crust thickness. Other data we know from the seismic model: thickness of sediments (or basement depth) and Moho depth (Fig. 5c, d). Magnetic crust thickness H_{MC} can be described by:

$$H_{MC} = \min\{H_{\text{Moho}}; H_{T_C}\} - H_{\text{Bas}}, \quad (8)$$

where H_{Moho} is Moho depth, H_{T_C} is Curie temperature (580 °C) depth and H_{Bas} is depth of basement (Fig. 13).

The maps of magnetic crust thickness H_{MC} calculated for Models A, B, C and D are shown in Fig. 13. All four maps are consistent and show clear differentiation of magnetic crust thickness: thin (< 25 km) for the south-west of TTZ, and thick (> 35 km) for NE Poland. In the central part of the Polish Basin magnetic crust thickness is only 5–10 km. This is because very thick non-magnetic sedimentary cover and shallow depth of Curie temperature. Also in Carpathians magnetic crust is thin (~20 km), which is mostly because of very thick sediments. Thick magnetic Precambrian and Cadomian crust (35–40 km) is a result of a great depth of Curie temperature, thick crust

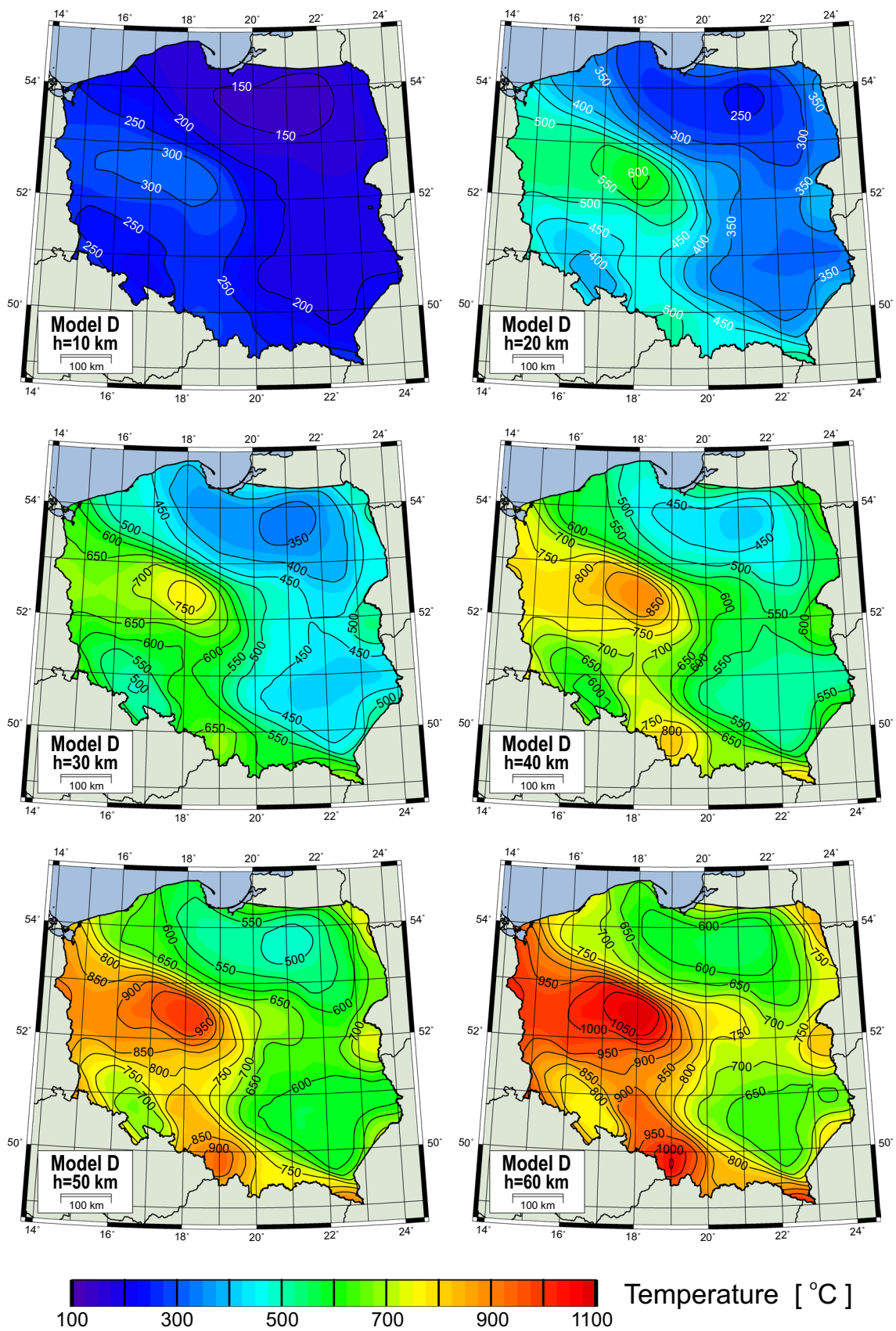


Fig. 11 Temperatures calculated for Model D at slices at depth of 10, 20, 30, 40, 50 and 60 km

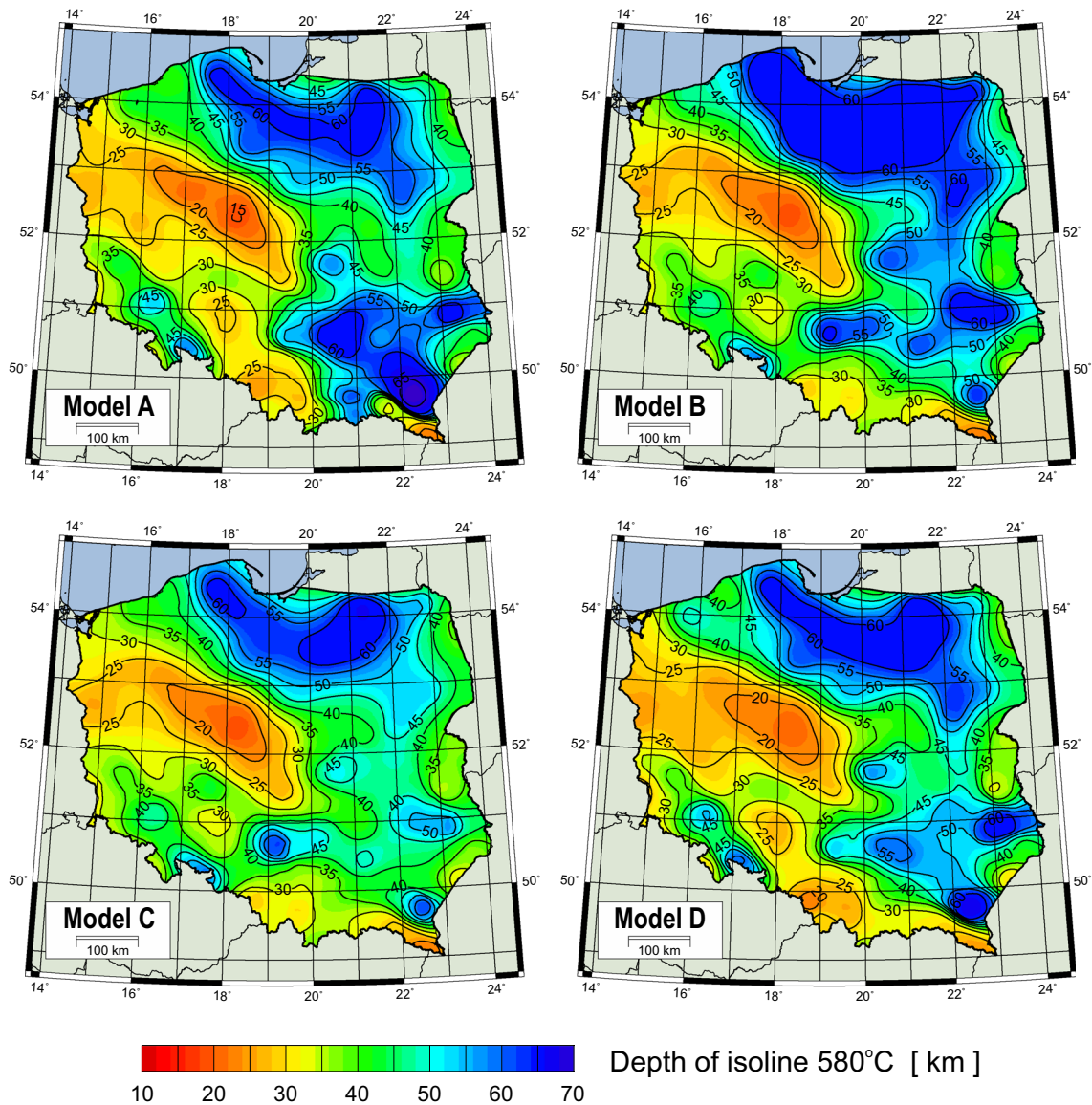


Fig. 12 Map of the Curie temperature ($T_C = 580\text{ }^\circ\text{C}$) depths calculated for Models A, B, C and D

and thin sediments. In Sudetes (SW Poland) magnetic crust is ~ 30 km due to very thin sediments.

Thermal LAB Thermal LAB depth Z_{LAB} has been calculated for four Models A, B, C and D (Fig. 14) according to formula (5). Depth to thermal LAB is determined from the depth of intersection of geotherm calculated for the last iteration (#5) with mantle adiabat $T_{\text{AD}}(z)$ as illustrated in the test results in Fig. 8 (Hyndman et al. 2009; MacKenzie and Canil 1999):

$$T_{\text{AD}}(z) = T(0) + 0.3 \cdot z \quad (9)$$

where $T(0) = 1300\text{ }^\circ\text{C}$, z is depth in km, and temperature gradient is $0.3\text{ }^\circ\text{C}/\text{km}$. Temperatures for depths 100 km and 200 km are $T(100) = 1330\text{ }^\circ\text{C}$ and $T(200) = 1360\text{ }^\circ\text{C}$,

respectively. However, this method for estimation the LAB depth is somewhat simplified and may be significantly more complex (see Eaton et al. 2009, for a review on the LAB). It gives an approximation to rather uncertain thermal data in the upper lithosphere.

Calculated for four Models A, B, C and D thermal LAB depths (Fig. 14) show large variability between Paleozoic Platform (90–120 km) and Precambrian and Cadomian units (> 150 km).

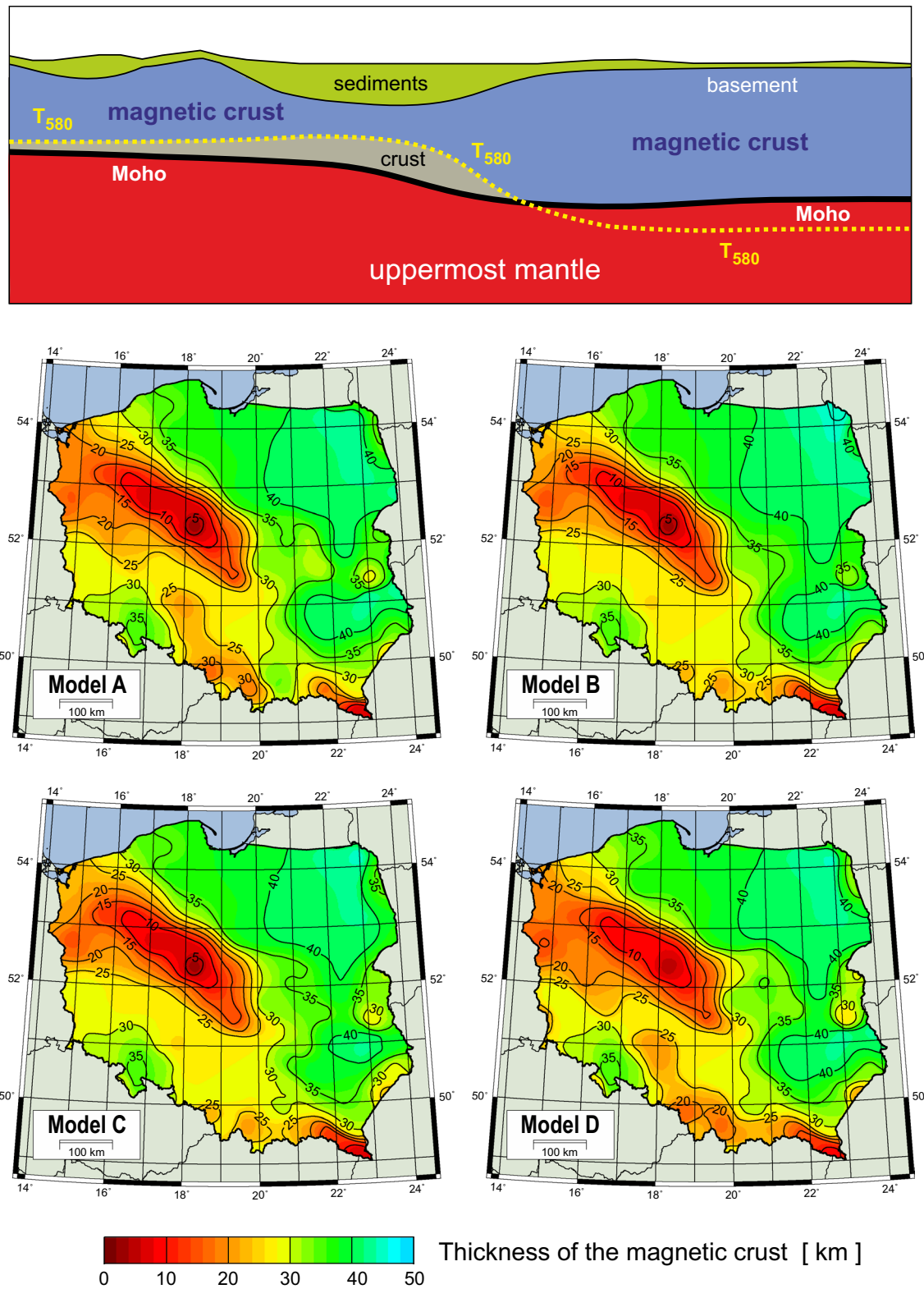


Fig. 13 Cartoon illustrating magnetic crust described by formula (8) and maps of the magnetic crust thickness calculated for Models A, B, C and D

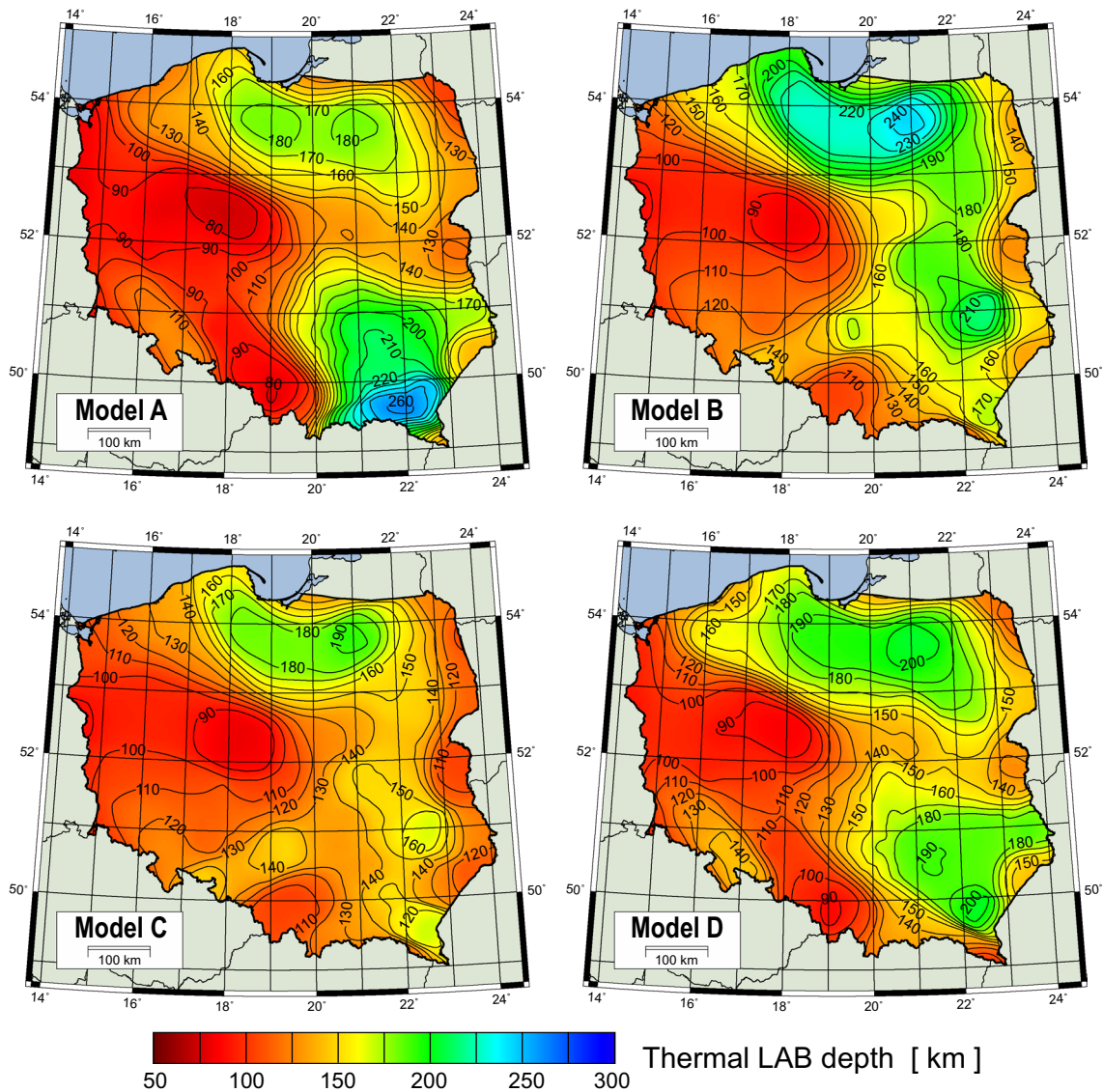


Fig. 14 Thermal LAB depth Z_{LAB} (in km) calculated from the observed surface heat flow Q_0 and assumed heat production and thermal conductivity data for four Models: A, B, C and D (compare parameters in Table 1)

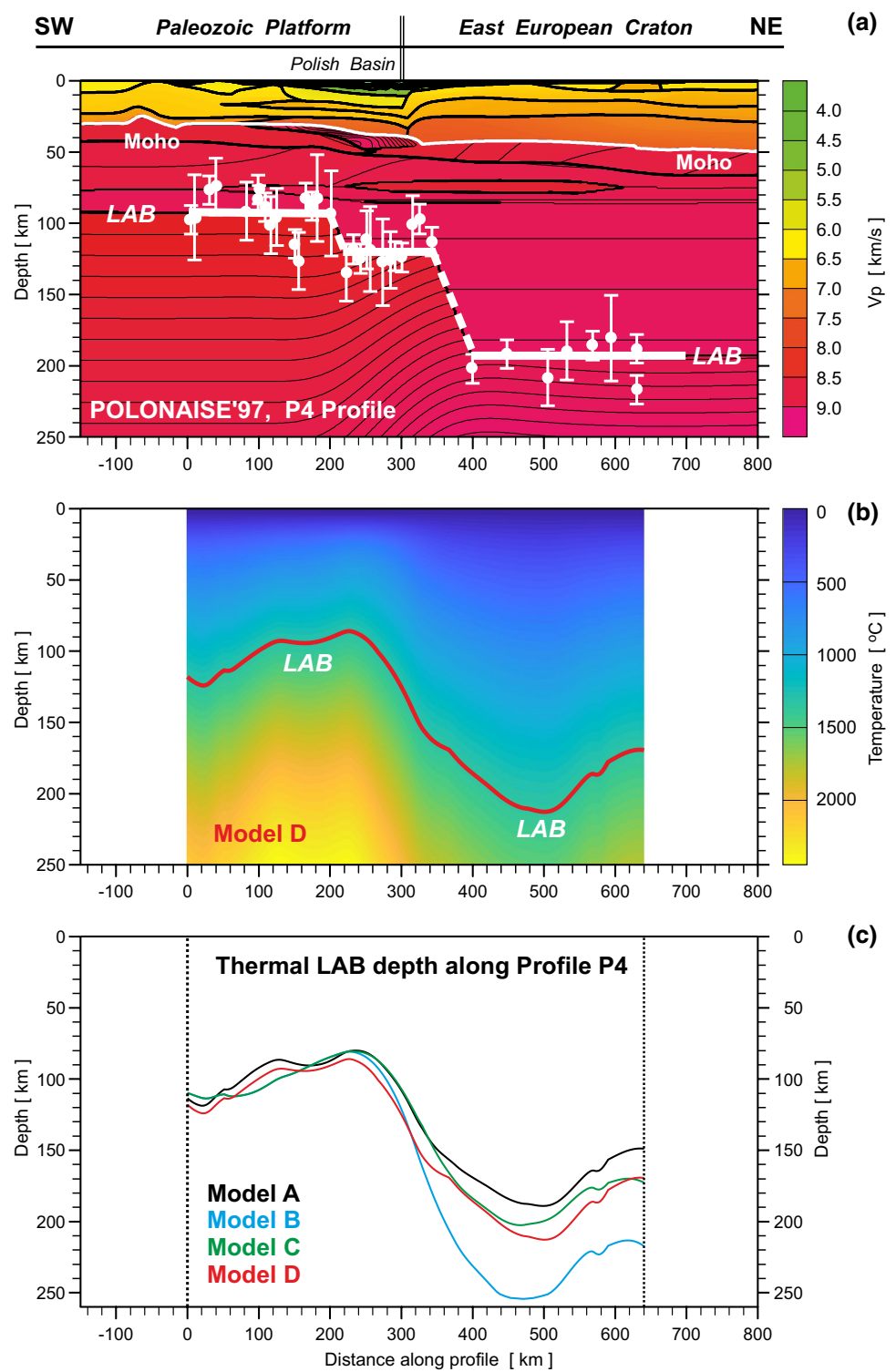
Thermal LAB and seismic LAB-comparison

The lithosphere–asthenosphere boundary LAB is not a sharp discontinuity, but rather a gradual and thick transition zone (see e.g. Meissner 1986). In seismology the asthenosphere was identified as a low-velocity channel in the 50–200 km depth range in Gutenberg’s global model of the Earth (Gutenberg 1959). Recently, the LAB depth have been effectively estimated by global and regional tomography (e.g. Gregersen et al. 2006; Pasyanos 2010). The LAB may also correlate with change in the anisotropy direction (e.g. Eaton et al. 2009; Plomerová and Babuška 2010). The asthenosphere could be identified as a low-viscosity zone and a low value of the quality factor, Q_S (e.g. Stacey 1969;

Karato 2010). Characteristic for asthenosphere is low seismic activity or even total lack of earthquakes. The electrically defined LAB is marked by a significant reduction in electrical resistivity, where resistive lithosphere is overlying the highly conductive asthenosphere (e.g. Eaton et al. 2009; Korja 2007; Jones et al. 2010). Different definitions and method estimations of LAB should be considered when comparing to thermal LAB.

Comparison with LAB along profile P4 Comparison of our thermal LAB depth variability calculated for four thermal models described above (Models A, B, C and D) with the independent seismological experiment data along the profile P4 shows general agreement within the errors of both methods (Fig. 15). Seismic model of the crust and

Fig. 15 Comparison of seismic and thermal LAB along profile P4. **a** Model of the crust and uppermost mantle beneath profile P4 down to 250 km depth (see Fig. 5b for location). White dots with error bars are LAB depths determined from relative P-residuals of teleseismic events and thick white lines are average LAB depths along profile (Wilde-Piórko et al. 2010). **b** Temperature and LAB depth for Model D. **c** Comparison of LAB depths calculated for Models A, B, C and D



uppermost mantle beneath profile P4 shows thin crust and lithosphere beneath Paleozoic Platform, and thick crust and lithosphere beneath East European Craton. Seismic LAB depth were determined from relative P-residuals of teleseismic events (Wilde-Piórko et al. 2010). Average seismic LAB depths are about 90 km beneath PP, about 120 km beneath

Polish Basin, and about 190 km beneath EEC (Fig. 15a). In Fig. 15b temperature down to 250 km depth is shown together with thermal LAB depth for Model D. We have an agreement with seismic LAB depth within standard deviation of ± 30 km. Thermal LAB depths calculated for Models A, B, C and D (Fig. 15c) clearly show convergence of results

for south of TTZ (distance along profile 0–300 km), where the differences are in a few kilometers only. Much bigger differences are observed beneath EEC (up to 60 km).

Comparison with global and regional LAB depths As mentioned earlier, the depth of LAB could be estimated different, depending on the method used. Here we compare our thermal LAB depths (Fig. 14) with global and regional LAB depths obtained by different methods (Fig. 16). For the area of Poland “Tesauro” map was extracted from thermal LAB model of European lithosphere (Tesauro et al. 2009). “Hamza” map was extracted from global thermal LAB map (Hamza and Vieira 2012). “Priestley” map was extracted

from global seismic LAB model (Priestley and McKenzie 2013), which was obtained using surface waves tomography. The fundamental and higher modes of Rayleigh surface waves (periods between 50 and 160 s) were used to image structures, with a horizontal resolution of ~250 km and a vertical resolution of ~50 km to depths of ~300 km in the upper mantle. “Seis-Grav” LAB depth map was compiled from regional seismic LAB data, mostly in northern Poland (blue dots) and from gravity LAB data, mostly in southern Poland (red dots). Seismic data were compiled from different seismic techniques: relative P-residuals of teleseismic events recorded along profile P4 (Wilde-Piórko et al. 2010),

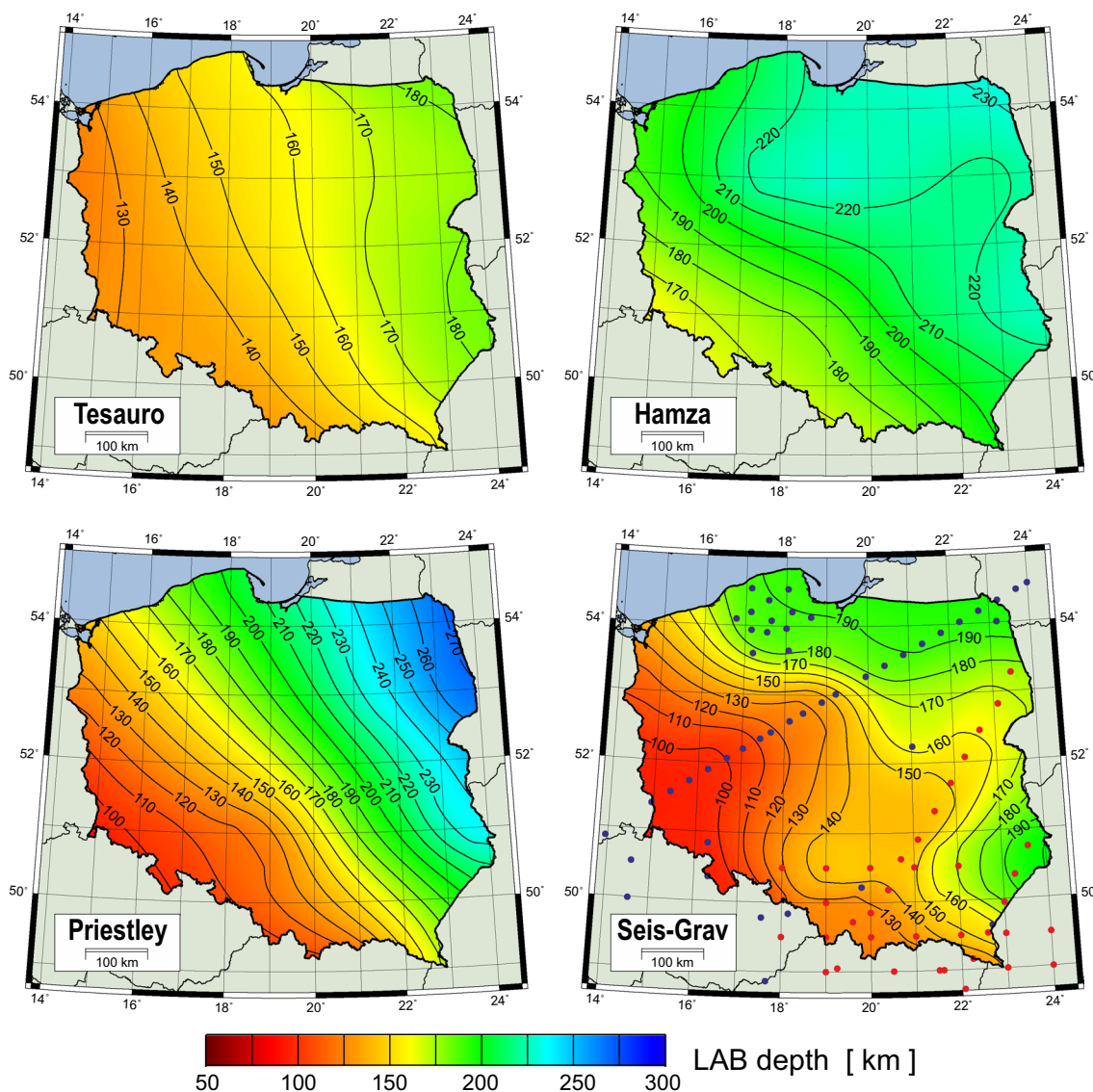


Fig. 16 Map of LAB depth for the area of Poland. “Tesauro” map is extracted from European thermal LAB map (Tesauro et al. 2009). “Hamza” map is extracted from global thermal LAB map (Hamza and Vieira 2012). “Priestley” map is extracted from global seismic LAB map (Priestley and McKenzie 2013). “Seis-Grav” map is com-

pared from regional seismic LAB data (blue dots), compiled from Wilde-Piórko et al. (2010), Geissler et al. (2010), Grad et al. (2015, 2018), and from gravity LAB data (red dots), compiled from Bielik (1999), Horváth et al. (2006) and Grabowska et al. (2011)

receiver function (Geissler et al. 2010), dispersion of surface waves (Grad et al. 2018). Gravity LAB depths were compiled from 2D gravity modeling (Bielik 1999; Bielik et al. 2006; Grabowska et al. 2011) and from regional map (Horváth et al. 2006).

All four LAB maps shown in Fig. 16 show in general decrease of depth from NE Poland towards SW Poland. However, all they differ in details. In the “Tesauro” map this decrease is from 180 to 130 km, with an almost constant gradient. These values are underestimated by about 20 km (compare geotherm in Fig. 8), because in this paper the LAB depth was assumed at isotherm of 1200 °C. In the “Hamza” map the LAB depth is relatively flat (210–230 km) for the EEC, decreasing to about 170 km with almost constant gradient in SW Poland. In the “Priestley” map decrease of LAB depth is the biggest: from 270 to 100 km, with gradient almost constant, but about three times bigger than in “Tesauro” map. All three maps have continental or global scale, so also their resolution is low. “Seis-Grav” LAB depth map is not so smooth as three models shown before. This is because local data were used, which better reflect local structure. For the EEC typical LAB depths are 170–190 km, for Cadomian unit and Carpathians 140–160 km, and 100–130 km for Paleozoic Platform. The boundaries between these units are more narrow gradients zones. For example, 40 km LAB depth change between PP and EEC (from 130 to 170 km) follows at distance of circa 100 km only.

Discussion and conclusions

We find large variability in heat flow Q_0 and calculated mantle heat flow Q_M (heat flow from below the crust) across Poland. An elevated mantle heat flow (circa 30–40 mW/m²) is typical in the Paleozoic Platform. It is some 20 mW/m² higher than Moho heat flow in the north-eastern and south-eastern Poland belonging to different tectonic terranes from the EEC, TESZ and Cadomian area in SE Poland (Fig. 9). Mantle heat flow variability is mainly correlating with measured surface heat flow and influences geotherms and depth point of their intersection with the mantle adiabat. Calculated thermal LAB depth follows patterns of heat flow and Moho heat flow variability through Poland with the thinnest lithosphere in the high mantle heat flow areas. Comparison of this thermal LAB depth estimates with seismic/gravity data based LAB shows general coincidences when EEC vs PP areas are considered (circa 190 km depth vs some 90 km depth, respectively) along the profile P4 seismic experiment data. General trend is basically the same. However, significant differences exist in many areas and especially for the SE Poland when comparison is made between thermal LAB depth maps with the compilation map from other

seismological and gravity LAB determinations (Fig. 16). We have thinned LAB in the SW Poland and thickest in parts of the craton and the difference in depth is some 100 km.

The lithosphere thinning mainly in the Paleozoic Platform with thicknesses as low as ~100 km found by the independent seismological data gives good confirmation of the validity of our assumptions in our thermal models. To have thinner thermal lithosphere in the Paleozoic Platform high heat flow zone requires higher mantle heat flow than in the thick lithosphere—low heat flow craton.

Heat flow and mantle heat flow calculations from our thermal models show that the main regional scale (~100 km scale) variability in heat flow from 45 to 55 mW/m² for the craton to 65–75 mW/m² for the Paleozoic Platform in Poland comes largely from some 20 mW/m² difference in the mantle heat flow between both areas. Upper crustal radiogenic contribution in the Paleozoic Platform younger consolidated crust is also larger than in the craton, however, the Precambrian crust is much thicker.

If to the contrary we were to assume thermal models in which the differences between heat flow for the Paleozoic Platform high heat flow and low heat flow for the craton come entirely from the differences in the upper crustal radiogenic heat production contribution to heat flow (higher for the Paleozoic Platform crust) then mantle heat flow would be pretty equal between the areas. However, in such case it would be impossible to have the model calculation to give us thinning of the thermal lithosphere, e.g. shallower thermal LAB under the high heat flow area shown by the independent seismological LAB depth estimates by several independent works (Fig. 16).

In the continental scale, the LAB depths in Poland correspond to the average depth values for Phanerozoic and Precambrian Europe. According to Jones et al. (2010) average seismic LAB depth for Phanerozoic Europe is 133 ± 49 km and for Precambrian Europe 182 ± 13 km. The TESZ is visible as a strong, step-like change of ~100 km of the depth to the LAB. This change is greater than the difference between the two mean values between Phanerozoic and Precambrian Europe. Electrically defined average LAB depth for Precambrian Europe is 66 km deeper, and for Phanerozoic Europe is 20 km shallower than corresponding seismic LAB (Jones et al. 2010). In the northern Europe, the LAB depth beneath Barents Sea was found at depth of circa 200 km (Grad et al. 2014). First arrivals of P-waves from local earthquakes show no evidence for “shadow zone” related to low velocity zone (asthenosphere), which could either be interpreted as the absence of the asthenosphere beneath the central part of the Baltic Shield, or that the LAB in this area occurs deeper than 200 km (Grad et al. 2014).

The inference of the thermal LAB is not trivial and comparison with lithosphere thickness inferred from other geophysical method is not so straightforward and generally

seismic determined LAB is commonly deeper than thermal LAB (Jaupart et al. 1998, Eaton et al. 2009; Artemieva 2011; Chiozzi et al. 2017). The depth difference between the thermally conductive layer and the top of the convective mantle found between our thermal LAB and that based on seismic tomography is not surprising. According to Jaupart et al. (1998) and Artemieva (2011) the difference can be as large as 40–50 km as there are differences between thermal and seismological lithosphere. For one, lithospheric temperature varies gradually with depth and the heat transfer gradually changes from conduction to convection. The thermal boundary between lithosphere and asthenosphere is transitional. For second, the surface waves tomography generally shows sharp boundary and velocity inversion boundary is generally at a depth greater than the thermal lithosphere–asthenosphere transition.

Temperature variations at Moho calculated for assumed thermal conductivity $\lambda(z)$ and heat production $A(z)$ for Models A, B, C and D show similar pattern with differences of about ± 50 °C only (Fig. 10). The lowest Moho temperature 400–500 °C is observed for Precambrian and Cadomian units and the highest Moho temperature 800–900 °C is observed in the area of Central Poland, which well correlates with the area of Polish Basin and continues towards the North-Eastern German Basin. Such temperature contrasts are observed also at depth slices (Fig. 11). Beneath the Paleozoic Platform temperatures are higher than beneath the Precambrian and Cadomian units: about 150 °C at 10 km, 300 °C at 20 km, about 400 °C at 50–60 km depth. This relatively big change occurs at distance spaced about 300 km only.

Differences in temperature influence depth of Curie temperature, here assumed as 580 °C (e.g. Gasparini et al. 1979). For all models results are consistent (Fig. 12), showing relatively shallow depth of T_C beneath the Paleozoic Platform, 15–30 km only, and much deeper, reaching 40–55 km beneath the Precambrian and Cadomian. This is also crucial for the magnetic crust thickness, which could have been calculated using thickness of sediments (or basement depth) and Moho depth. Magnetic crust thickness is thin for the south-west of TTZ (< 25 km), and thick for NE Poland (> 35 km). In the central part of the Polish Basin magnetic crust thickness is only 5–10 km. Shallow Curie temperature and thin magnetic crust of the Paleozoic Platform should be taken into consideration in magnetic modeling (e.g. Petecki 2002).

Our thermal modeling of the lithosphere for the area of Poland shows consistent results for the temperature, heat flow at Moho, magnetic crust and LAB depth. We observe differences in results, and our preferred model is Model D (see Table 1). In this model, we used properties of 3D seismic model (geometry, V_p velocity, tectonic division) and local thermal data (conductivity λ and heat production A).

The spatial variability of modelled mantle heat flow and thickness of the lithosphere, in general correlates with measured surface heat flow. These thermally modelled characteristics of the lithosphere–asthenosphere relationships reflect the transient nature of heat flow related to variability in lower mantle heat input and radiogenic heat production of the crust and mainly of the upper crust. The radiogenic heat producing isotopes of U, Th and K of the crust have been assembled over millions–billions of years. Observed low heat flow, low mantle heat flow and thick thermal lithosphere are related not just to the craton east of the TTZ but also to the Cadomian crust in SE Poland (Fig. 4). Cadomian orogeny, which occurred on the margin of the Gondwana continent is related to series of events in the late Neoproterozoic, about 650–550 Ma (Karnkowski 2008). They occurred in southern Poland and also in several other areas of Europe, including northern France, the English Midlands, southern Germany, Bohemia. Relatively thick lithosphere we get for our models for the Precambrian Craton east of TTZ is also present in the Cadomian units and partly within the Caledonian Pomeranian Massif (see Fig. 4). All of these areas of thick lithosphere and low mantle heat flow are related to low to moderate heat flow < 60 mW/m². Thinner lithosphere (< 100 km) is mainly in high heat flow > 70 mW/m², observed in the marginal zone of VDF (see Fig. 1). When, considering that the latest volcanism in that area within the Permian basin is old 290–270 million years (Karnkowski 2008) the remnant heat of the rifting basinal extensional phase must have been long dissipated considering diffusivity dependent cooling time constant (Jessop and Majorowicz 1994). To the South-Western Poland volcanism is much younger and of Cenozoic ages, 30 and 18 million years age (Puziewicz et al. 2012, 2017, Puziewicz et al., manuscript in revision). It could be speculated that the thinning of the lithosphere and crust are still a result of quite ancient deeply seated (> 150 km) magmatic event which may have been going through a stage of later deep rejuvenation (failed mantle plume?). When comparing lithospheric thinning, heat flow and mantle heat flow of the studied here area of Poland with Pannonian basin or Rhine Graben it shows that our research area cooled down much more and it is consistent with tectonic age differences.

Age dependence of terrestrial heat flow was statistically evaluated for the relevant heat flow and tectonic age world data in the different tectonic settings in the past (e.g. Jessop 1990). The relationship of heat flow Q , with time t , is of the form $Q(t) = C \cdot t^{-b}$, for continents and $Q(t) = C \cdot t^{-1/2}$ for ocean basins. The inverse relationship between heat flow and the square root of crustal age matches theoretically predicted one-dimensional lithospheric cooling models (Crough and Thompson 1976). There is also half-time decay factor for radiogenic elements in the crust (Jessop 1992). In the older Precambrian cratons of billion years of age, radiogenic

heat production be less due to radiogenic decay of U, Th, K. These factors play significant role to explain low heat flow—thick lithosphere of some 1 Gy years old craton in comparison with much younger regions of magmatically rejuvenated in Cenozoic older Variscan Platform to south west of TTZ. Relatively low heat flow—thick lithosphere in the northern Carpathian foreland area in Poland is in contrast to high heat flow and thinned lithosphere in the inner zone (Pannonian basin) which fits heat flow vs tectonic age general relationship and is related to much older crust beneath foreland.

The heat flow and temperature maps for the area of Poland as shown in this paper can be found in digital form at: <https://www.igf.fuw.edu.pl/pl/informations/zaklad-fizyki-litosfery-igf-fuw-67954/>.

Acknowledgements This study was possible thanks to the National Science Centre Poland (NCN) project DEC-2011/02/A/ST10/00284. The public domain GMT software (Wessel and Smith 1991, 1998) has been used to produce maps.

OpenAccess This article is distributed under the terms of the Creative Commons Attribution 4.0 International License (<http://creativecommons.org/licenses/by/4.0/>), which permits unrestricted use, distribution, and reproduction in any medium, provided you give appropriate credit to the original author(s) and the source, provide a link to the Creative Commons license, and indicate if changes were made.

References

- Aichroth B, Prodehl C, Thybo H (1992) Crustal structure along the Central Segment of the EGT from seismic-refraction studies. *Tectonophysics* 207:43–64
- Artemieva IM (2011) *The lithosphere: an interdisciplinary approach*. Cambridge University Press, New York
- Artemieva IM, Mooney WD (2001) Thermal thickness and evolution of Precambrian lithosphere: a global study. *J Geophys Res* 106(B8):16387–16414
- Bała M, Waliczek M (2012) Radiogenic heat of Zechstein and Carboniferous rocks calculated using well-logging data from the Brońsko. Reef area *Prz Geol* 60:155–163
- Balling N (1995) Heat flow and thermal structure of the lithosphere across the Baltic Shield and northern Tornquist Zone. *Tectonophysics* 244:13–50
- Bayer U, Grad M, Pharaoh TC, Thybo H, Guterch A, Banka D, Lamarche J, Lassen A, Lewerenz B, Scheck M, Marotta A-M (2002) The southern margin of the East European Craton: new results from seismic sounding and potential fields between the North Sea and Poland. *Tectonophysics* 360:301–314
- Berthelsen A (1992) From Precambrian to Variscan Europe. In: Blundell DJ, Freeman R, Mueller, St (eds) *A continent revealed—the European geotraverse*. Cambridge University Press, Cambridge, pp 153–164
- Bielik M (1999) Geophysical features of the Slovak Western Carpathians: a review. *Geol Q* 43(3):251–262
- Bielik M, Kloska K, Meurers B, Švancara J, Wybraniec S, Fancsik T, Grad M, Grand T, Guterch A, Katona M, Królikowski C, Mikuška J, Pašteka R, Petecki Z, Polechońska O, Ruess D, Szalaiová V, Šefara J, Vozár J (2006) Gravity anomaly map of the CELEBRATION 2000 region. *Geol Carpath* 57(3):145–156
- Blackwell DD, Steele JL (1989) Heat flow and geothermal potential of Kansas. *Kansas Geol Surv Bull* 226:267–295
- Bogdanova S, Gorbatschev R, Grad M, Janik T, Guterch A, Kozlovskaya E, Motuza G, Skridlaite G, Starostenko V, Taran L, EUROBRIDGE and POLONAISE Working Groups (2006) EUROBRIDGE: new insight into the geodynamic evolution of the East European Craton. In: Gee DG, Stephenson RA (eds) *European lithosphere dynamics*. Geological Society, London, pp 599–625 (**Memoirs 32**)
- Bruneton M, Pedersen HA, Farra R, Arndt NT, Vacher P, Achauer U, Alinaghi A, Ansoorge J, Bock G, Friedrich W, Grad M, Guterch A, Heikkinen P, Hjelt SE, Hyvonen TL, Ikonen JP, Kissling E, Komminaho K, Korja A, Kozlovskaya E, Nevsky MV, Paulssen H, Pavlenkova NI, Plomerova J, Raita T, Riznichenko OY, Roberts RG, Sandoval S, Sanina IA, Sharov NV, Shomali ZH, Tiikainen J, Wielandt E, Wylegalla K, Yliniemi J, Yurov YG (2004) Complex lithospheric structure under the central Baltic Shield from surface wave tomography. *J Geophys Res* 109:B10303
- Cacace M, Scheck-Wenderoth M, Noack V, Cherubini Y, Schellschmidt R (2013) Modelling the surface heat flow distribution in the area of Brandenburg (northern Germany). *Energy Procedia* 40:545–553
- Čermák V, Bodri L (1986) Temperature structure of the lithosphere based on 2D temperature modelling, applied to central and eastern Europe. In: Burrus J (ed) *Thermal modeling in sedimentary basins: 1st IFP Exploration Research Conference, Carcans, France, June 3–7, 1985*. Collection Colloques Et Seminaires, 44, Imprint Paris, pp 7–31 (**Editions Technip**)
- Čermák V, Šafanda J, Guterch A (1989) Deep temperature distribution along three profiles crossing the Teisseyre–Tornquist tectonic zone in Poland. *Tectonophysics* 164:151–163
- Chapman DS, Furlong KP (1992) Thermal state of the continental lower crust. In: Fountain DM, Arculus R, Kay RW (eds) *Continental lower crust*. Elsevier, Amsterdam, pp 179–199
- Chiozzi P, Barkaoui A, Rimi A, Zarhloule Y (2017) A review of surface heat-flow data of the northern Middle Atlas (Morocco). *J Geodyn* 112. <https://doi.org/10.1016/j.jog.2017.10.003>
- Chmura K (1970) *Własności fizyko-termiczne skał niektórych polskich zagłębi górniczych*. Wyd Śląsk, Katowice (**in Polish**)
- Chmura K (1987) *Własności cieplne skał górotworu Górnośląskiego Zagłębia Węglowego*. In: *Metody i środki eksploatacji na dużych głębokościach*. Pr MGIE 119, Pol Śląska, Gliwice (**in Polish**)
- Clark SP Jr (ed) (1966) *Handbook of physical constants*, Geol Soc America Mem 97, p 587
- Correia A, Šafanda J (2002) Geothermal modelling along a two-dimensional crustal profile in Southern Portugal. *J Geodyn* 34:47–61
- Crough ST, Thompson GA (1976) Thermal model of continental lithosphere. *J Geophys Res* 81:4857–4862
- Cymerman Z (2007) Does the Mazury dextral shear zone exist? *Prz Geol* 55:157–167 (**in Polish with English abstract**)
- Czuba W, Grad M, Luosto U, Motuza G, Nasedkin V, POLONAISE P5 Working Group (2001) Crustal structure of the East European Craton along POLONAISE '95 P5 profile. *Acta Geoph Pol* 49:145–168
- Dadlez R, Grad M, Guterch A (2005) Crustal structure below the Polish Basin: Is it composed of proximal terranes derived from Baltica? *Tectonophysics* 411:111–128
- Dortman NB (ed) (1976) *Physical properties of rocks mineral deposits (petrophysics)*. Handbook geophysics. Nedra, Moscow (**in Russian**)
- Downorowicz S (1983) Geotermika złoża rud miedzi monokliny przed-sudeckiej. *Pr Inst Geol* 106

- Eaton DW, Darbyshire F, Evans RL, Grütter H, Jones AG, Yuan X (2009) The elusive lithosphere–asthenosphere boundary (LAB) beneath cratons. *Lithos* 9:1–22
- Eppelbaum L, Kutasov I, Pilchin A (2014) Thermal properties of rocks and density of fluids. In: Applied geothermics, lecture notes in earth system sciences. Springer, Berlin, pp 99–149
- EUROBRIDGE'95 Seismic Working Group, Yliniemi J, Tiira T, Luosto U, Komminaho K, Giese R, Motuza G, Nasedkin V, Jacyna J, Seckus R, Grad M, Czuba W, Janik T, Guterch A, Lund C-E, Doody JJ (2001) EUROBRIDGE'95: deep seismic profiling within the East European Craton. *Tectonophysics* 339:153–175
- Franke W (2014) Topography of the Variscan orogen in Europe: failed—not collapsed. *Int J Earth Sci* 103:1471–1499
- Gąsior I, Przelaskowska A (2012) Application of statistic method for determination radiogenic heat of meso-paleozoic rocks fore-Carpathian region Tarnów—Dębica (Wykorzystanie metod statystyki matematycznej do oceny ciepła radiogenicznego skał mezopaleozoicznych zapadliska przedkarpackiego rejonu Tarnów—Dębica). *Nafta-Gaz* 68(7):411–420 (in Polish)
- Gasparini P, Mantovani MSM, Corrado G, Rapolla A (1979) Depth of Curie temperature in continental shields: a compositional boundary? *Nature* 278:845–846
- Geissler WH, Sodoudi F, Kind R (2010) Thickness of the central and eastern European lithosphere as seen by S receiver functions. *Geophys J Int* 181:604–634
- Górecki W (ed) (2006) Atlas of geothermal resources of Mesozoic formations in the Polish Lowlands. Ministry of the Environment, ZSE AGH, Kraków (in Polish)
- Grabowska T, Bojdys G, Bielik M, Csicsay K (2011) Density and magnetic models of the lithosphere along CELEBRATION 2000 profile CEL01. *Acta Geophys* 59(3):526–560
- Grad M (1991) Seismic wave velocities in the sedimentary cover of the Palaeozoic platform in Poland. *Bull Pol Acad Earth Sci* 39(1):13–22
- Grad M, Polkowski M (2016) Seismic basement in Poland. *Int J Earth Sci* 105:1199–1214
- Grad M, Trung Doan T, Klimkowski W (1990) Seismic models of sedimentary cover of the Precambrian and Palaeozoic platforms in Poland. *Kwart Geol* 34:393–410 (in Polish with English abstract)
- Grad M, Janik T, Yliniemi J, Guterch A, Luosto U, Tiira T, Komminaho K, Środa P, Höing K, Makris J, Lund C-E (1999) Crustal structure of the mid-Polish trough beneath the TTZ seismic profile. *Tectonophysics* 314:145–160
- Grad M, Guterch A, Mazur S (2002a) Seismic refraction evidence for crustal structure in the central part of the Trans-European Suture Zone in Poland. In: Winchester JA, Pharaoh TC, Verniers J (eds) Palaeozoic amalgamation of central Europe. Geological Society, London, pp 295–309 (Special Publications 201)
- Grad M, Keller GR, Thybo H, Guterch A, POLONAISE Working Group (2002b) Lower lithospheric structure beneath the Trans-European Suture Zone from POLONAISE '97 seismic profiles. *Tectonophysics* 360:153–168
- Grad M, Jensen SL, Keller GR, Guterch A, Thybo H, Janik T, Tiira T, Yliniemi J, Luosto U, Motuza G, Nasedkin V, Czuba W, Gaczyński E, Środa P, Miller KC, Wilde-Piórko M, Komminaho K, Jacyna J, Korabliova L (2003) Crustal structure of the Trans-European suture zone region along POLONAISE'97 seismic profile P4. *J Geophys Res* 108(B11):2541
- Grad M, Guterch A, Polkowska-Purys A (2005) Crustal structure of the Trans-European Suture Zone in Central Poland—re-interpretation of the LT-2, LT-4 and LT-5 deep seismic sounding profiles. *Geol Q* 49:243–252
- Grad M, Guterch A, Keller GR, Janik T, Hegedűs E, Vozár J, Ślaczka A, Tiira T, Yliniemi J (2006) Lithospheric structure beneath trans-Carpathian transect from Precambrian platform to Pannonian basin: CELEBRATION 2000 seismic profile CEL05. *J Geophys Res* 111:B03301
- Grad M, Guterch A, Keller GR, POLONAISE'97 and CELEBRATION 2000 Working Groups (2007) Variations in lithospheric structure across the margin of Baltica in Central Europe and the role of the Variscan and Carpathian orogenies. *Geol Soc Am Memoir* 200:341–356
- Grad M, Guterch A, Mazur S, Keller GR, Špičák A, Hrubcová P, Geissler WH (2008) Lithospheric structure of the Bohemian Massif and adjacent Variscan belt in central Europe based on profile S01 from the SUDETES 2003 experiment. *J Geophys Res* 113:B10304
- Grad M, Tiira T, ESC Working Group (2009) The Moho depth map of the European plate. *Geophys J Int* 176:279–292
- Grad M, Tiira T, Olsson S, Komminaho K (2014) Seismic lithosphere–asthenosphere boundary beneath the Baltic Shield. *GFF* 136:581–598
- Grad M, Polkowski M, Wilde-Piórko M, Suchcicki J, Arant T (2015) Passive seismic experiment “13 BB star” in the margin of the East European Craton, Northern Poland. *Acta Geophys* 63:352–373
- Grad M, Polkowski M, Ostaficzuk SR (2016) High-resolution 3D seismic model of the crustal and uppermost mantle structure in Poland. *Tectonophysics* 666:188–210
- Grad M, Puziewicz J, Majorowicz J, Chrapkiewicz K, Lepore S, Polkowski M, Wilde-Piórko M (2018) The geophysical characteristic of the lower lithosphere and asthenosphere in the marginal zone of the East European Craton. *Int J Earth Sci* 107:2711–2726
- Gregersen S, Voss P, Shomali ZH, Grad M, Roberts RG, TOR Working Group (2006) Physical differences in the deep lithosphere of Northern and Central Europe. In: Gee DG, Stephenson RA (eds) European lithosphere dynamics. Geological Society, London, pp 313–322 (Memoirs 32)
- Gregersen S, Wiejacz P, Dębski W, Domański B, Assinovskaya BA, Guterch B, Mäntyniemi P, Nikulin VG, Pacesa A, Puura V, Aronov AG, Aronova TI, Grünthal G, Husebye ES, Sliupa S (2007) The exceptional earthquakes in Kaliningrad district, Russia on September 21, 2004. *Phys Earth Planet Inter* 164(1–2):63–74
- Gutenberg B (1959) *Physics of the Earth's Interior*. Academic Press, New York
- Guterch A, Grad M, Materzok R, Toporkiewicz S (1983) Structure of the Earth's crust of the Permian basin in Poland. *Acta Geophys Pol* 31(2):121–138
- Guterch A, Grad M, Janik T, Materzok R, Luosto U, Yliniemi J, Lück E, Schulze A, Förste K (1994) Crustal structure of the transition zone between Precambrian and Variscan Europe from new seismic data along LT-7 profile (NW Poland and eastern Germany). *C R Acad Sci Paris* 319:1489–1496
- Guterch A, Grad M, Thybo H, Keller GR, POLONAISE Working Group (1999) POLONAISE'97—an international seismic experiment between Precambrian and Variscan Europe in Poland. *Tectonophysics* 314:101–121
- Guterch A, Grad M, Keller GR, Posgay K, Vozár J, Špičák A, Brückl E, Hajnal Z, Thybo H, Selvi O, CELEBRATION 2000 Working Group (2003) CELEBRATION 2000 seismic experiment. *Stud Geophys Geod* 47:659–669
- Guterch A, Grad M, Keller GR, Brückl E (2015) Crustal and lithospheric structure between the Alps and East European Craton from long-range controlled source seismic experiments. In: Schubert G, Romanowicz B, Dziewonski A (eds) *Treatise on geophysics*, 2nd edn, vol. 1. Elsevier, Amsterdam, pp 557–586 (Deep Earth Seismology)
- Hamza VM, Vieira FP (2012) Global distribution of the lithosphere–asthenosphere boundary: a new look. *Solid Earth* 3:199–212

- Hasterok D, Chapman DS (2011) Heat production and geotherms for the continental lithosphere. *Earth Planet Sci Lett* 307(1–2):59–70
- Horváth F, Bada G, Windhoffer G, Csontos L, Dombárdi E, Dövényi P, Fodor L, Grenczy Gy, Síkhegyi F, Szafián P, Székely B, Tímár G, Tóth L, Tóth T (2006) Atlas of the present-day geodynamics of the Pannonian basin: Euroconform maps with explanatory text. *Magyar Geofizika* 47(4):133–137
- Hrubcová P, Šroda P, CELEBRATION 2000 Working Group (2008) Crustal structure at the easternmost termination of the Variscan belt based on CELEBRATION 2000 and ALP 2002 data. *Tectonophysics* 460:55–75
- Hyndman RD, Currie CA, Mazzotti S, Frederiksen A (2009) Temperature control of continental lithosphere elastic thickness, T_e vs V_s . *Earth Planet Sci Lett* 277:539–548
- Janik T, Yliniemi J, Grad M, Thybo H, Tiira T, POLONAISE P2 Working Group (2002) Crustal structure across the TESZ along POLONAISE'97 seismic profile P2 in NW Poland. *Tectonophysics* 360:129–152
- Janik T, Grad M, Guterch A, Dadlez R, Yliniemi J, Tiira T, Gaczyński E, CELEBRATION 2000 Working Group (2005) Lithospheric structure of the Trans-European Suture Zone along the TTZ & CEL03 seismic profiles (from NW to SE Poland). *Tectonophysics* 411:129–155
- Janik T, Grad M, Guterch A, CELEBRATION 2000 Working Group (2009) Seismic structure of the lithosphere between the East European Craton and the Carpathians from the net of CELEBRATION 2000 profiles in SE Poland. *Geol Q* 53(1):141–158
- Janik T, Grad M, Guterch A, Vozár J, Bielik M, Vozárova A, Hegedűs E, Kovács CS, Kovács I, Keller GR, CELEBRATION 2000 Working Group (2011) Crustal structure of the Western Carpathians and Pannonian Basin: seismic models from CELEBRATION 2000 data and geological implications. *J Geodyn* 52:97–113
- Jaupart C, Mareschal J-C (2003) Constraints on crustal heat production from heat flow data. In: Rudnick R (ed) *Treatise on geochemistry: the crust*, ch 2, vol 3. Elsevier, Amsterdam, pp 65–84
- Jaupart C, Mareschal JC, Guillou-Frottier L, Davaille A (1998) Heat flow and thickness of the lithosphere in the Canadian Shield. *J Geophys Res Solid Earth* 103(7):15269–15286
- Jensen SL, Janik T, Thybo H, POLONAISE Working Group (1999) Seismic structure of the Palaeozoic Platform along POLONAISE'97 profile P1 in NW Poland. *Tectonophysics* 314(1–3):123–144
- Jessop AM (1990) *Thermal geophysics. Developments in solid earth geophysics*. Elsevier, Amsterdam
- Jessop AM (1992) Thermal input from the basement of the Western Canada Sedimentary Basin. *Bull Can Pet Geol* 40:198–206
- Jessop A, Majorowicz JA (1994) Heat transfer in sedimentary basins. In: Parnell J (ed) *Geofluids: origin, migration and evolution of fluids in sedimentary basins*, 78. *Geol Soc Spec Publ*, Geological Society, London, pp 43–54
- Jones AG, Plomerova J, Korja T, Sodoudi F, Spakman W (2010) Europe from the bottom up: A statistical examination of the central and northern European lithosphere–asthenosphere boundary from comparing seismological and electromagnetic observations. *Lithos* 120:14–29
- Kappelmeyer O, Hänel R (1974) Geothermics with special reference to application. *Geoexploration Mon Ser*, vol 1, no 4. Gebrueder Borntraeger, Berlin
- Karato S (2010) Rheology of the Earth's mantle: a historical review. *Gondwana Res* 18:17–45
- Karnkowski PH (2008) Tectonic subdivision of Poland: Polish lowlands. *Prz Geol* 56:895–903 (**in Polish with English abstract**)
- Korja T (2007) How is the European lithosphere imaged by magnetotellurics? *Surv Geophys* 28:239–272
- Królikowski C (2006) Crustal-scale complexity of the contact zone between the Palaeozoic Platform and the East European Craton in the NW Poland. *Geol Q* 50(1):33–42
- Lenkey L, Dövényi P, Horváth F, Cloetingh SAPL (2002) Geothermics of the Pannonian basin and its bearing on the Neotectonics. *EGU Stephan Mueller Spec Publ Ser* 3:29–40
- MacKenzie JM, Canil D (1999) Composition and thermal evolution of cratonic mantle beneath the central Archean Slave Province, NWT, Canada. *Contrib Mineral Petrol* 134:313–324
- Maj S (1991) Geothermal gradients in the Baltic Shield lithosphere. *Acta Geophys Pol* 47(4):411–422
- Majdański M, Grad M, Guterch A, SUDETES 2003 Working Group (2006) 2-D seismic tomographic and ray tracing modelling of the crustal structure across the Sudetes Mountains basing on SUDETES 2003 experiment data. *Tectonophysics* 413:249–269
- Majorowicz J (1978) Mantle heat flow and geotherms for major tectonic units in Central Europe. *Pure Appl Geophys* 117:107–124
- Majorowicz JA (2004) Thermal lithosphere across the trans-European suture zone in Poland. *Geol Q* 48(1):1–14
- Majorowicz J, Plewa S (1979) Study of heat flow in Poland with special regard to tectonophysical problems. In: Čermák V, Rybach L (eds) *Terrestrial heat flow in Europe*. Springer, Berlin, Heidelberg, pp 240–252
- Majorowicz J, Wybraniec S (2011) New terrestrial heat flow map of Europe after regional paleoclimatic correction application. *Int J Earth Sci* 100(4):881–887
- Majorowicz J, Čermák V, Šafanda J, Krzywiec P, Wróblewska M, Guterch A, Grad M (2003) Heat flow models across the Trans-European suture zone in the area of the POLONAISE'97 seismic experiment. *Phys Chem Earth* 28:375–391
- Malinowski M, Żelaźniewicz A, Grad M, Guterch A, Janik T (2005) Seismic and geological structure of the crust in the transition from Baltica to Palaeozoic Europe in SE Poland—CELEBRATION 2000 experiment, profile CEL02. *Tectonophysics* 401:55–77
- Mazur S, Mikołajczak M, Krzywiec P, Malinowski M, Buffenmyer V, Lewandowski M (2015) Is the Teisseyre-Tornquist Zone an ancient plate boundary of Baltica? *Tectonics* 34:2465–2477
- Meissner R (1986) The continental crust—a geophysical approach. *International Geophysics Series*, Academic Press Inc, Orlando
- Moisiejev UO, Smyslov AA (1986) *Temperature of the Earth's interior*. Nedra, Leningrad (**in Russian**)
- Narkiewicz M, Grad M, Guterch A, Janik T (2011) Crustal seismic velocity structure of southern Poland: preserved memory of a pre-Devonian terrane accretion at the East European Platform margin. *Geol Mag* 148:191–210
- Norden B, Förster A, Balling N (2008) Heat flow and lithospheric thermal regime in the Northeast German Basin. *Tectonophysics* 460(1–4):215–229
- Pasyanos ME (2010) Lithospheric thickness modeled from long-period surface wave dispersion. *Tectonophysics* 481:38–50
- Petecki Z (2002) Gravity and magnetic modelling along the seismic LT-7 Profile. *Przegl Geol* 50(7):630–633
- Pharaoh TC (1999) Palaeozoic terranes and their lithospheric boundaries within the Trans European Suture Zone (TESZ): a review. *Tectonophysics* 314:17–41
- Plewa M (1988) Wyniki badań ciepła radiogenicznego skał obszaru Polski (The results of radiogenic heat investigations for the rocks in the area of Poland). *Zeszyty Naukowe AGH, Geofizyka Stosowana* 1:109–122 (**in Polish**)
- Plewa S (1994) Distribution of geothermal parameters on the territory of Poland. *Publications of the Center for basic problems of mineral raw materials and energy management*. Polish Acad Sci, Kraków, pp 1–38

- Plewa M, Plewa S (1992) *Petrofizyka (Petrophysics)*. Wyd Geol, Warszawa, p 327 **(in Polish)**
- Plomerová J, Babuška V (2010) Long memory of mantle lithosphere fabric—European LAB constrained from seismic anisotropy. *Lithos* 120:131–143
- Polkowski M, Grad M (2015) Seismic wave velocities in deep sediments in Poland: borehole and refraction data compilation. *Acta Geophys* 63(3):698–714
- Pollack HN (1986) Cratonization and thermal evolution of the mantle. *Earth Planet Sci Lett* 80:175–182
- Pollack HN, Chapman DS (1977) Mantle heat flow. *Earth Planet Sci Lett* 34:174–184
- Pozaryski W, Dembowski Z (1983) Geological map of Poland and neighboring countries without Cenozoic, Mesozoic and Permian deposits (1:1000000). Geol Inst, Warsaw
- Priestley K, McKenzie D (2013) The relationship between shear wave velocity, temperature, attenuation and viscosity in the shallow part of the mantle. *Earth Planet Sci Lett* 381:78–91
- Puziewicz J, Czechowski L, Krysiński L, Majorowicz J, Matusiak-Malek M, Wróblewska M (2012) Lithospheric thermal structure at the eastern margin of the Bohemian Massif: a case petrological and geophysical study of the Niedźwiedź amphibolite massif (SW Poland). *Int J Earth Sci* 101:1211–1228
- Puziewicz J, Polkowski M, Grad M (2017) Geophysical and petrological modeling of the lower crust and uppermost mantle in the Variscan and Proterozoic surroundings of the Trans-European Suture Zone in Central Europe. *Lithos* 276:3–14
- Rabbel W, Förste K, Schulze A, Bittner R, Röhl J, Reichert JC (1995) A high-velocity layer in the lower crust of the North German Basin. *Terra Nova* 7:327–337
- Rudnick R, Gao S (2003) Composition of the continental crust. In: Rudnick R (ed) *Treatise on geochemistry: The Crust*, ch 1, vol 3. Elsevier, Amsterdam, pp 1–64
- Rybach L (1976) Radioactive heat production in rocks and its relation to other petrophysical parameters. *Pure Appl Geophys* 114:309–318
- Rybach L (1978) The relationship between seismic velocity and radioactive heat production in crustal rocks: an exponential law. *Pure Appl Geophys* 117:75–82
- Rybach L, Buntebarth G (1984) The variation of heat generation density and seismic velocity with rock type in the continental crust. *Tectonophysics* 103:309–344
- Schweitzer J (1995) Blockage of regional seismic waves by the Teisseyre-Tornquist Zone. *Geophys J Int* 123:260–276
- Sharma PV (2002) *Environmental and engineering geophysics*. Cambridge University Press, Cambridge
- Skridlaitė G, Bogdanova S, Page L (2006) Mesoproterozoic events in eastern and central Lithuania as recorded by $^{40}\text{Ar}/^{39}\text{Ar}$ ages. *Baltica* 19:91–98
- Sokołowski J (1968) Geology and structure of the regional units of Poland from the point of view oil exploration. *Surowce Mineralne* 1:7–58 **(in Polish)**
- Sokołowski J (1992) *Geosynoptical atlas of Poland*. MEERI, Polish Acad Sci, Kraków **(52 charts)**
- Środa P, POLONAISE Working Group (1999) P- and S-wave velocity model of the southwestern margin of the Precambrian East European Craton; POLONAISE'97, profile P3. *Tectonophysics* 314:175–192
- Środa P, Czuba W, Grad M, Guterch A, Tokarski AK, Janik T, Rauch M, Keller GR, Hegedűs E, Vozár J, CELEBRATION 2000 Working Group (2006) Crustal and upper mantle structure of the Western Carpathians from CELEBRATION 2000 profiles CEL01 and CEL04: seismic models and geological implications. *Geophys J Int* 167:737–760
- Stacey FD (1969) *Physics of the Earth*. Wiley, New York
- Starostenko V, Janik T, Kolomiyets K, Czuba W, Środa P, Grad M, Kovács I, Stephenson R, Lysynchuk D, Thybo H, Artemieva IM, Omelchenko V, Gintov O, Kutas R, Gryn D, Guterch A, Hegedűs E, Komminaho K, Legostaeva O, Tiira T, Tolkunov A (2013) Seismic velocity model of the crust and upper mantle along profile PANCAKE across the Carpathians between the Pannonian Basin and the East European Craton. *Tectonophysics* 608:1049–1072
- Teisseyre W (1893) *Całokształt płyty palaeozoicznej Podola Galicyjskiego. Rzecz o przyszłych wierceniach głębokich na Podolu opolskim*. Kosmos Lwów 18:310–336 **(in Polish)**
- Tesauro M, Kaban MK, Cloetingh SAPL (2009) A new thermal and rheological model of the European lithosphere. *Tectonophysics* 476(3–4):478–495
- Tornquist A (1908) Die Feststellung des Südwesttrendes des baltisch-russischen Schildes und die geotektonische Zugehörigkeit der ost-preussischen Scholle. *Schr Phys Ökon Ges Königsberg* 49(1):1–12
- Wessel P, Smith WHF (1991) Free software helps map and display data. *EOS Trans Am Geophys Union* 72(41):445–446
- Wessel P, Smith WHF (1998) New, improved version of generic mapping tools released. *EOS. Trans Am Geophys Union* 79(47):579
- Wilde-Piórko M, Grad M, TOR Working Group (2002) Crustal structure variation from the Precambrian to Palaeozoic platforms in Europe imaged by the inversion of teleseismic receiver functions—project TOR. *Geophys J Int* 150:261–270
- Wilde-Piórko M, Świeczak M, Grad M, Majdański M (2010) Integrated seismic model of the crust and upper mantle of the Trans-European Suture zone between the Precambrian Craton and Phanerozoic terranes in Central Europe. *Tectonophysics* 481:108–115
- Winchester JA, PACE TMR Network Team ((2002) Palaeozoic amalgamation of Central Europe: new results from recent geological and geophysical investigations. *Tectonophysics* 360:5–21
- Wróblewska M, Majorowicz J (2008) Opracowanie modeli termicznych litosfery obszaru SE Polski. In: Grad M, Guterch A (eds) *Kompleksowa interpretacja anomalii pól potencjalnych wzdłuż wszystkich profili głębokich badań refrakcyjnych zrealizowanych na całym obszarze CELEBRATION 2000*. Arch Ministry of Environment, Warsaw
- Zeb A, Firdous T, Maqsood A (2010) Thermophysical properties of dunite rocks as a function of temperature along with the prediction of effective thermal conductivity. *Nat Sci* 2(6):626–630
- Ziegler PA (1990) *Geological atlas of western and central Europe*, 2nd edn. Shell Internationale Petroleum Maatschappij BV, Den Haag
- Zielhuis A, Nolet G (1994) The deep seismic expression of an ancient plate boundary in Europe. *Science* 265:79–81